Organized Crime, Hidden Pollution, and Long-Run Health Costs*

Davide Cipullo†
Massimiliano Gaetano Onorato‡
Gianmario Pelleschi§

This version: April 28, 2026

First version: October 2025

Abstract

We study the long-run health effects of illegal toxic waste disposal conducted by organized crime in Italy. We exploit quasi-random variation in historical wind direction around contaminated sites combined with a difference-in-differences design. Using administrative data on cancer deaths spanning four decades, we find that wind exposure to pollutants increases the number of cancer deaths substantially. The effects emerge after long latencies and grow over time. In later years, wind exposure implies roughly two additional cancer deaths per municipality-year relative to unexposed municipalities equally proximate to contaminated sites. Our findings reveal a previously unmeasured health externality of organized crime.

Keywords: Organized crime; Environmental externalities; Pollution and health; State capacity; Cancer mortality.

JEL classification: K42; Q53; I18; D62

*We are grateful to Alberto Bisin, Pietro Biroli, Giovanni Mastrobuoni, Francesca Calamunci, Lorenzo Cappellari, Augustìn Casas, Giulia Caprini, Felipe Carozzi, Tommaso Colussi, Amanda Dahlstrand, Roberto Dellisanti, Gianluca Femminis, Claudio Ferraz, Davide Furceri, Federico Franzoni, Caterina Gennaioli, Marco Le Moglie, Marco Ovidi, Flaviana Palmisano, Elias Papaioannou, Eugenio Polese, Alessio Romarri, Matteo Sandi, Emiliano Santoro, Sandra Sequeira, Jakob Svensson, Federico Trombetta, as well as seminar participants at Cattolica University of Milan WIP Political Economy Seminar Series, the 2025 Sustainability Environmental Economics and Dynamics Studies (SEEDS) Annual Conference, the "Inequalities and Opportunities (insights into wealth, income and education disparities)" Conference at the University of Bari, and the 37^{th} Annual Congress of the Italian Society of Public Economics (SIEP) held in Naples. We gratefully acknowledge the Regional Agency for the Protection of the Environment Campania (ARPAC) for granting access to the environmental data. All remaining errors are our own.

†Department of Economics and Finance, Università Cattolica del Sacro Cuore, Milan, Italy; CESifo, Munich, Germany; Uppsala Centre for Fiscal Studies, Uppsala University, Sweden; CIFREL, Milan, Italy. Email: davide.cipullo@unicatt.it

‡Department of Economics, University of Bologna, Bologna, Italy. Email: massimiliano.onorato@unibo.it

§Department of Economics and Finance, Università Cattolica del Sacro Cuore, Milan, Italy; CIFREL, Milan, Italy. Email: gianmario.pelleschi@unicatt.it

1 Introduction

Economic activity often generates environmental externalities, but these are typically studied in settings where emissions are regulated, observable, and at least partially recorded (e.g., Jacobsen et al., 2023; Schlenker and Walker, 2016; Yang et al., 2024; Zou, 2021). Much less is known about the environmental harm generated by illegal activities, where pollution is deliberately concealed and regulatory enforcement is weak. In such contexts, standard regulatory tools fail, exposure is difficult to detect, and the resulting health costs may remain invisible for long periods. As a consequence, the social costs of illegal activities may be substantially underestimated.

Organized crime is a particularly relevant case. Beyond distorting markets, politics, and public spending (e.g., Acconcia et al., 2014; Acemoglu et al., 2020; Fenizia and Saggio, 2024; Mirenda et al., 2022), criminal organizations often engage in activities that generate severe environmental damage, such as the illegal disposal and burning of hazardous waste. These activities are highly profitable because they bypass regulation and monitoring, and their consequences are difficult to trace back to the perpetrators. Affected populations may remain unaware for years of their exposure to pollution produced in this way, while environmental and health damage accumulates over time.

This paper studies the long-term health implications of illegal disposal of toxic waste perpetrated by criminal organizations in the *Terra dei Fuochi* (Land of Fires), a densely populated area in the South of Italy. Since the late 1980s, criminal organizations have systematically buried, dumped, and burned hazardous industrial waste, often imported from other regions and countries. These operations were highly profitable and carefully concealed, involving the underground disposal of toxic materials during construction works and the burning of accumulated waste in unregulated open-air fires. Unlike legal industrial emissions, these activities were neither monitored nor recorded. Local residents remained largely unaware of the risks they faced for at least fifteen years after criminal organizations started the illegal disposal of toxic waste.[1]

We exploit quasi-random variation in historical wind direction around contaminated sites and a difference-in-differences design that relies on detailed death count data spanning 1980–2022. Our results document that wind exposure to pollutants stemming from the contaminated sites increases the number of cancer deaths substantially. Specifically, estimates that refer to the later years of our sample period suggest that municipalities exposed to pollutants experience on average two additional cancer deaths per year (corre-

[1] A multidisciplinary literature provides correlational evidence about the environmental and epidemiological conditions of the *Terra dei Fuochi*, documenting an association between the concentration of pollutants and increased risks of cancer and other diseases (e.g., Alberti et al., 2022; Italian National Institute of Health (Istituto Superiore di Sanità), 2019; Marfè et al., 2024; Mazza et al., 2015). Beraldo et al. (2026) estimate a cross-sectional association between the estimated risk of cancer mortality and the presence of criminal organizations, as proxied by seized assets and the dissolution of municipal administrations due to mafia infiltration.

sponding to several hundred additional deaths per year across the affected area) relative to unexposed municipalities. These effects emerge only after long latencies, grow over time, and persist for decades. They are consistent with exposure to toxic pollutants that accumulate over the years. Our estimates are relatively homogeneous across types of cancer although they are primarily concentrated among diseases that the epidemiological literature associates with a prolonged exposure to pollutants. Exposure to toxic waste increases the number of deaths among individuals aged 01-19. This finding is consistent with previous evidence suggesting that the health consequences of exposure to pollution on fragile demographic groups may extend beyond an increase in the incidence of tumor (Alexander and Schwandt, 2022; Chay and Greenstone, 2003; Currie and Neidell, 2005; Currie et al., 2009; Klauber et al., 2024).

Our paper links the literature on organized crime with that on environmental and health economics and documents a new channel through which organized crime harms welfare. On the one hand, a large body of research in economics has shown how criminal organizations affect economic growth (Fenizia and Saggio, 2024; Pinotti, 2015), firm performance (Calamunci and Drago, 2020; Mirenda et al., 2022; Slutzky and Zeume, 2024) and creation (Le Moglie and Sorrenti, 2022), the allocation of public spending (Acconcia et al., 2014; Di Cataldo and Mastrorocco, 2022), political representation (Acemoglu et al., 2020; Alesina et al., 2019; Daniele and Geys, 2015), and even educational outcomes (Sviatschi, 2022).[2] On the other hand, a large and rigorous literature in environmental and health economics has shown that exposure to pollutants—whether through air, soil, or water—can substantially increase mortality and morbidity (e.g., Aggeborn and Öhman, 2021; Chay and Greenstone, 2003; Currie and Neidell, 2005; Currie et al., 2009; Deryugina et al., 2019; Isen et al., 2017) especially among the more fragile demographic groups (e.g., Alexander and Schwandt, 2022; Bishop et al., 2023; Hollingsworth and Rudik, 2021; Klauber et al., 2024). However, these works typically examine emissions from regulated industrial production, transportation, energy generation, or accidental releases. Despite the prominence of environmental crime in public debates, we lack credible causal evidence in economics on whether organized crime generates persistent health harm to the population. Our work fills this gap by credibly showing that criminal activities can also impose long-run health costs on the general population. Because pollution generated by illegal activities is hidden by design, these costs are unlikely to be internalized through market mechanisms or addressed by standard environmental policy, amplifying the welfare losses associated with weak enforcement capacity. We also make a number of contributions to this area of research. First, compared to the existing work, our results allow us to quantify to what extent cancerous diseases contribute to the overall impact of pollution on the number of deaths and to separately identify the effects across various types of

[2] Gennaioli and Tavoni (2016) provide empirical evidence that publicly subsidized renewable energy can attract investments by criminal organizations.

cancer and age groups. Second, our results focus on a prolonged and persistent exposure to pollutants which spans several decades. Third, our data, that cover a prolonged time span, allow us to evaluate the effect of hidden pollution on cancer deaths although cancerous diseases develop after long latencies since the exposure to pollutants and take an even longer time to eventually cause the death of the patient.

2 Background and Institutional Context

Starting in the late 1980s, organized crime groups operating in Southern Italy developed a large-scale illegal waste disposal business that served Italian and sometimes foreign firms. Due to the substantial costs implied by the legal treatment, transportation, and documentation of hazardous industrial waste, criminal organizations provided an alternative channel that dramatically reduced costs bypassing treatment requirements, falsifying documents, and avoiding regulatory oversight altogether.

From an economic perspective, illegal waste disposal emerged as a high-margin criminal service. On the demand side, manufacturing firms faced strong incentives to minimize disposal costs in a context characterized by uneven enforcement and limited monitoring capacity. On the supply side, criminal organizations could exploit territorial control, corruption, and intimidation to operate disposal sites without interference. Thus, the logic governing this activity differed from that of legal waste management or regulated industrial production. Disposal decisions were driven by concealment and cost minimization rather than by technological or environmental constraints. As a result, waste was frequently buried or burned in locations selected for their invisibility rather than their suitability, often in close proximity to residential areas, agricultural land, and water sources.

The focus of this paper is on the illegal disposal activities concentrated in an area of the Campania region in the South of Italy that mainly encompasses municipalities in the provinces of Naples and Caserta.[3] The area is characterized by an exceptionally high population density, fragmented land use, and a mixture of residential, agricultural, and light industrial zones. Disposal sites were not concentrated in a small number of fixed locations but were small and numerous, spatially dispersed, and located within inhabited areas. Illegal dumping occurred on agricultural land, along roads, near construction sites, and in abandoned quarries. Open-air burning was frequently used to reduce waste volume, generating airborne emissions that could travel beyond the immediate vicinity of disposal sites. The widespread use of intentional wildfires to destroy toxic waste is the

[3]Italy has three sub-national levels of government. From the top to the bottom these are the regions (20), the provinces (approximately 110, nested within regions), and municipalities ($\approx$ 8,000, nested within provinces). The Campania region is divided in 5 provinces (Naples, Avellino, Benevento, Caserta, and Salerno) and 550 municipalities.

reason why, in the popular debate and on the Italian press, the area is mainly known as the *Terra dei Fuochi* (Land of Fires).[4]

The illegal dumping of waste was one of the main businesses of the criminal organization operating in the area (the *Casalesi*). Although the exact time when this criminal organization started this activity is difficult to establish, it is reasonable to think that it was around the mid-80s.[5] The illegal disposal of toxic waste soon became one of their main businesses. Illegal waste disposal took mainly two forms: burial and open-air burning. Burial often occurred during construction projects, when hazardous materials were concealed beneath roads, buildings, or other infrastructure. Burning was used both to destroy waste directly and to reduce the volume of materials prior to burial.[6] Fires were typically unregulated and uncontrolled, releasing pollutants directly into the atmosphere. Burial can contaminate soil and groundwater in the exact location of the disposal, leading to persistent environmental exposure through agricultural production and water use. Moreover, burning releases airborne pollutants that disperse according to the prevailing wind conditions in the atmosphere and, in turn, may affect individuals' health either through direct exposure or through contamination of soil and water away from the disposal site.

A defining feature of the *Terra dei Fuochi* is that illegal disposal activities were deliberately concealed and mostly took place in proximity to the *Casalesi*'s headquarters in the town of Casal di Principe. Environmental authorities lacked records of disposal sites, emissions were not monitored, and the existence, timing, and composition of dumped waste were largely unknown to local residents for many years. Although rumors and isolated reports circulated, systematic investigations began only in the late 1990s and early 2000s, well after large-scale dumping had taken place.[7] This informational setting had two important implications for our analysis. First, households could not respond contemporaneously to pollution risks through avoidance behavior or migration, limiting

[4]The name *Terra dei Fuochi* appeared in 2003 in a report of a non-profit pro-environment organization. Nowadays, also official government reports use this name to denote the area. The Italian Government recognizes 90 municipalities as being a part of the *Terra dei Fuochi* due to the intensity of contaminated sites in their territory. Municipalities included in this list are reported in black in Figure A1 in the Appendix.

[5]One of former leaders of the criminal organizations operating in the area, Carmine Schiavone, started to co-operate with the judicial authority and the police in 1993. The detailed accounts provided by Mr. Schiavone are the main source of information about the affected areas, the quantity of illegally buried waste, and the variety of dispersed materials. According to Mr. Schiavone's hearing before the Italian House of Deputies (Italian House of Deputies, 1997), the activity was organized by the criminal group since 1988 although some actions were committed by members of the criminal organizations a few years before. Mr. Schiavone reports that his group processed several million tons of waste over the period 1988–1992.

[6]As the business was growing faster than the available land and rumors about the activity grew, waste was also abandoned in open areas (creating, thus, illegal dump facilities) and burned to minimize the needed volume and space.

[7]In 1998, the Minister for the Environment included the area as a part of the top national priorities for drainage from pollution together with localities around large petrol and metal plants.

endogenous sorting during the initial exposure period. Second, policy responses were delayed and incomplete due to the impossibility of monitoring and incomplete knowledge about the exact location of disposal sites. Even after the problem was officially recognized, cleanup efforts addressed only around 10 percent of contaminated sites, and most of the locations remain officially classified as "potentially contaminated" due to the absence of formal verification.[8] Toxic waste is still disposed of and burned in the area. Italian Ministry of Internal Affairs (2023) estimates that around 1,000 illegal fires of waste occurred in 2022, compared to an average of 2,000 fires per year in the previous decade and approximately 4,000 per year until 2013.

The pollutants involved in the illegal disposal of waste included substances characterized by environmental persistence and bioaccumulation, such as dioxins and heavy metals. Medical research indicates that cancers associated with exposure to these substances often develop after long latency periods, sometimes spanning decades.[9] Moreover, contamination of soil and water implies that exposure may continue long after disposal activities cease. These features motivate our focus on long-run outcomes and dynamic treatment effects. Unlike settings where pollution shocks are short-lived or sharply defined in time, individuals living in the *Terra dei Fuochi* are experiencing persistent exposure to pollutants over time paired with delayed manifestation of health consequences. As a result, short-term analyses would substantially understate the true health impact of illegal disposal activities.

3 Empirical strategy

3.1 Identification of Illegal Disposal Sites

We identify Illegal Disposal Sites (IDS) starting from the list of Potentially Contaminated Sites (PCS) published by the Campania Regional Agency for the Protection of the Environment (ARPAC). The first inventory was conducted in 2005 and the list was subsequently expanded in later years. As anticipated in Section 2, sites are labeled as "potentially" contaminated because a formal verification of each site has never been performed. Yet, the inclusion of a site in the inventory is subject to evidence of excessive concentration of pollutants on surface, subsoil, or groundwater. Since updates to the ARPAC list likely reflect recent discoveries of earlier disposal episodes, our analysis fo-

[8] At the beginning of the XXI century, the Italian government and the regional administration started careful investigations to identify areas at high risk of serious exposure to pollution. The Italian government estimates that only 10 percent of the potentially contaminated surface has been inspected, and that evidence of contamination has been found in approximately 70 percent of the inspected sites.

[9] Since 2006, the Italian National Institute of Health has compared the incidence of cancer diseases in the area affected by the illegal waste disposal with that of the rest of Italy. The latest estimates, published in 2025, indicate an excess mortality of approximately 1,600 individuals per year compared to the rest of the country.

cuses on the most comprehensive available version of the list.

The list of PCS includes information on the type of pollutant, the presumed activity there performed, and the exact geo-location of the site. We use the textual information provided in the list to exclude all sites that are related to legal activities such as production facilities, petrol suppliers, and legal dumps. The final list of Illegal Disposal Sites (IDS) that we use in our analysis includes 1,667 sites. Figure A1 reports the geographical distribution of the IDS in our sample. Most IDS are located in the municipalities officially recognized by the Italian government as a part of the *Terra dei Fuochi* (in black in the figure) although a non-negligible number of sites have been detected in other areas of the region.

3.2 Measuring wind-based exposure to illegal disposal sites

A key challenge to estimate the causal effect of exposure to pollutants generated by illegal waste disposal on the number of cancer deaths is that illegal disposal sites (IDS) are not randomly located. Municipalities closer to contaminated areas may differ systematically from those farther away. Therefore, a simple comparison of municipalities close vs. far from IDS risks confounding the effect of exposure with potentially unobservable differences in socioeconomic characteristics, crime presence, and health outcomes.

Our identification strategy exploits quasi-random variation in the atmospheric dispersion of pollutants driven by the prevailing historical wind direction. When hazardous waste is burned, airborne pollutants travel along wind trajectories. If wind patterns mainly blow from the IDS to the municipality (i.e., the municipality is downwind relative to the IDS), the municipality is systematically more likely to be exposed to pollutants than if wind blows from the municipality to the IDS (i.e., the municipality is upwind relative to the IDS). Therefore, our empirical analysis compares municipalities that are similarly close to disposal sites but differ in their exposure because of wind patterns.[10] This section provides details about the measurement of wind directions at each site and explains our strategy to measure exposure of municipalities to each polluting site. We refer the reader to Appendix B for a description of all the data sources and to Table A1 and Table A2 for the descriptive statistics of all variables.

We approximate historical wind directions at each IDS by combining information on the geographic location of each site and wind trajectory data from the 47 meteorological stations located in the Campania region (see Figure C2).[11] If winds predominantly blow

[10] Anecdotal evidence from Carmine Schiavone's reports and investigations from the judiciary indicate that wind patterns were not among the determinants that the criminal organization used to take into account when choosing where to locate disposal sites.

[11] As described in Appendix B, our wind direction data are only available since 2001. We document in Appendix C that alternative data that are available for a longer time span such as the Copernicus Climate Data Store's UERRA regional reanalysis for Europe approximate wind patterns imprecisely at the level of granularity that is necessary for our paper.

in a given direction, pollutants that are released when waste is burned are likely to be transported along that direction. Specifically, for each illegal disposal site s, meteorological station j and day τ, we retain station-day observations only when the wind observed at j on date τ blows towards s. Then, for each (s, j, τ) such that the wind observed at j of day τ blows towards s, we identify the five nearest stations to the site and compute the weighted average of wind directions measured at each station where weights reflect the inverse of the distance between s and j. This yields an estimated daily wind direction at each s, from which we calculate the historical mean wind direction at each s. Appendix C provides the details of the procedure. For each IDS, we then identify municipalities within a fixed distance and classify them as downwind or upwind based on the angle between the vector connecting the site to the municipality and the prevailing wind direction originating from the site.[12] In our main analysis, we consider municipalities located within a radius of 3 kilometers, consistently with the epidemiological literature that studies residential exposure to dioxins emissions from combustion sources (Chen et al., 2025; Praud et al., 2025; Rhee et al., 2023; VoPham et al., 2020). As a robustness check, we provide evidence that our results are larger in magnitude for small geographical distance radii and then decay when focusing on municipalities farther away from IDS.

Figure 1 offers a visualization of our approach considering a site and three municipalities (A, B, and C) that lie inside the fixed-area distance radius. In the example, wind blows from North-West to South-East (i.e., the direction of the arrow represents the wind direction). That is, municipalities B and C should not be exposed through wind to the pollutants stemming from the site. Municipality A, instead, lies inside the half-space defined by the line orthogonal to the wind direction and passing through the IDS; therefore, it is plausible that pollutants originating from the IDS will reach municipality A.

3.3 Empirical specifications

As discussed above, we calculate the total number of IDS within a fixed-radius distance from each municipality in Campania and, for each of them, whether the municipality is located downwind or upwind. Our main treatment variable $DownWind_i$ is the share of IDS relative to which the municipality is located downwind. Figure A3 in the Appendix documents that the treatment variable is orthogonal to a variety of municipal-level characteristics which importantly include measures of criminal activity, taxable income, meteorological and geographical characteristics, other sources of exposure to pollutants, and the municipality's population.

[12] As explained in Appendix D, we geo-locate each municipality taking into account that the urban center, which is relevant to measure whether individuals who live in a municipality may be affected by the pollutants stemming from an IDS does not usually coincide with the geometrical centroid of the municipality's shape. To this end, we construct a "demographic centroid" that locates each municipality based on the within-municipality distribution of the population across census blocks ($\approx$ 40 blocks per municipality).

Figure 1: Example of municipality's wind exposure to IDS

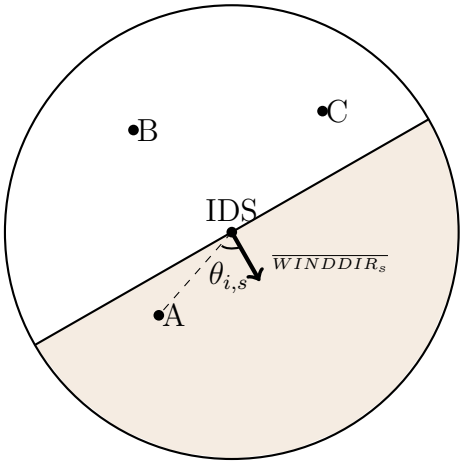

Notes: This figure illustrates how each municipality is classified as downwind relative to the Illegal Disposal Site (IDS), following Qiu et al. (2024). This occurs when the angle ($\theta_{i,s}$) between the connection vector (dashed line from the IDS to the municipality) and the historical average wind direction calculated at the IDS ($\overline{WINDDIR_s}$) falls within the range $[0°, 90°]$. In the figure, municipality A lies downwind while municipalities B and C are upwind. The downwind region (shaded area) is the half-space defined by a line orthogonal to the wind direction and passing through the IDS. Of the municipalities that lie near to the IDS, this classification allows us to isolate the subset of IDS that are likely to transmit pollutants towards the municipality's population.

We measure the health impact of wind exposure to pollutants stemming from IDS using administrative registry data on the number of deaths by municipality and cause of death, available yearly through the National Institute of Statistics (ISTAT) from 1980.[13] Our main dependent variable is the total number of deaths caused by malignant tumors. We do not rescale the dependent variable by the size of the municipality's population to ensure that our results really capture changes in the risk of death rather than changes in population size due to other channels potentially affected by exposure to pollutants, such as migration patterns or birth rates. Nevertheless, we show that municipalities exposed to differential wind trajectories are on statistically indistinguishable population growth rate patterns and that our results hold when including population growth rate as well as initial population interacted with municipality fixed effects as a control variable.

Our data allow us to measure cancer deaths over a long time horizon encompassing periods after the exposure to toxic waste and for several periods arguably before the exposure to pollutants started. This allows us to control for the municipality fixed effects (which account for all municipal-level observable and unobservable characteristics that are constant over time) and year fixed effects (which account for all observable and

[13]We cannot obtain data on cancer diagnoses by municipality-year. However, we argue that estimating an effect of wind exposure on cancer mortality would reflect also an underlying effect of wind exposure on cancer incidence. The reason is that municipalities in our sample are all part of the same health authority – in Italy, the healthcare system is mainly publicly funded and the management is conducted by regional governments. Thus, individuals living in different municipalities get access to the same preventive care, facilities, treatment, and doctors.

unobservable shocks common to all municipalities of the Campania region in a certain year). Specifically, we estimate a Difference-in-Differences (DiD) model on a panel of municipalities that spans the years 1980–2022.[14] Formally, we estimate the following equation:

$$y_{i,t} = DownWind_i \times \sum_{k=1980, k\neq 1987}^{2022} \beta_k \times \mathbf{1}(k=t) + \boldsymbol{X_i} \times \sum_{k=1980, k\neq 1987}^{2022} \gamma_k \times \mathbf{1}(k=t) + \eta_i + \delta_t + \varepsilon_{i,t}, \tag{1}$$

In equation (1), $\boldsymbol{X_i}$ is a vector of time-constant or pre-determined controls which we interact with year fixed effects to reassure about the validity of our design. Importantly for our purposes, the vector $\boldsymbol{X_i}$ includes a control for the total number of IDS located within the same fixed distance radius from the municipality.[15] This allows us to mimic the ideal experiment of comparing two municipalities exposed to the same number of IDS, but such that one municipality happens to be downwind relative to more IDS than the other municipalities. η_i is the municipality fixed effect and δ_t is the year fixed effect. $\varepsilon_{i,t}$ is the error term, robust to heteroskedasticity and clustering at the municipality level.

The coefficients of interest are $\beta_{1980,\ldots,2022}$. We treat the year 1987 as the reference category because repentant mafioso Carmine Schiavone reports that the *Casalesi* criminal organization dismissed toxic waste in a systematic manner since 1988. Moreover, cancer diseases due to toxic pollutants take time to develop and eventually cause death (Bertazzi et al., 2001). Based on these arguments, we argue that 1987 can be safely considered a pre-treatment year.

As discussed by Callaway et al. (2024), Difference-in-Differences designs with continuous treatment variable require imposing a stronger version of the parallel-trends assumption compared to binary-treatment cases if one aims to identify "average causal responses" (i.e., the causal effect of marginal changes in treatment intensity). To this end, one should be willing to assume that parallel trends hold across every possible treatment dosage.[16] Importantly, this stronger parallel trends assumption cannot be violated if the continuous treatment variable is exogenous – which sounds plausible in this context since we are leveraging relative wind paths between each IDS and each municipality. Indeed, as described above, plausible exogeneity of historical wind trajectories is reassured

[14] Our unit of observation is a municipality as of 1980 boundaries. To improve comparability, we exclude the five provincial capitals from our main analysis. As documented in Appendix E, including them does not affect our conclusions.

[15] The vector $\boldsymbol{X_i}$ also includes municipality surface area, number of civilians killed by the Mafia, minimum altitude, wind speed and rainfall, an indicator for dissolution due to Mafia infiltration, baseline census population (1981), and province fixed effects.

[16] Under the standard parallel trends assumption between untreated units and treated units it is still possible to identify the difference in outcomes between municipalities with zero exposure and those with (any level of) positive exposure.

Figure 2: Wind Exposure to Land of Fires Pollutants and Cancer Deaths

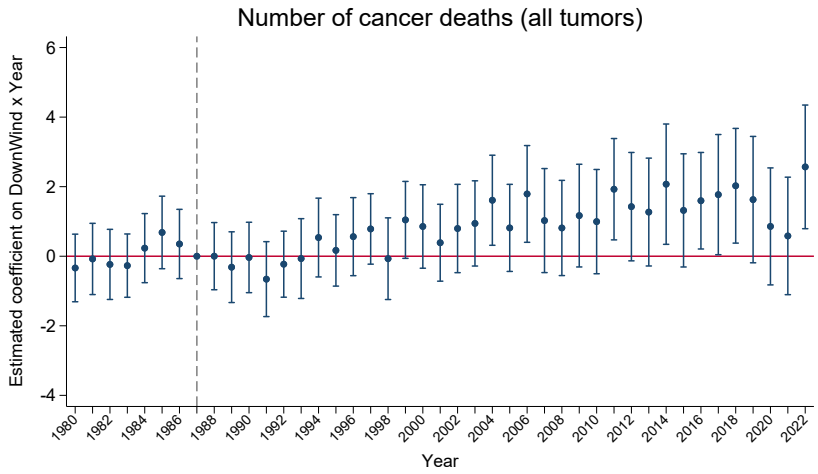

Notes: This figure reports coefficients for $\beta_{1980,\ldots,2022}$ in equation (1). Coefficient β_{1987} is omitted as it is considered the reference year. Estimated equation is (1). The dashed gray vertical line (1987) marks the omitted year. 95% confidence intervals are based on standard errors robust to clustering at the municipality level.

by the balancing exercise performed in Figure A3.[17]

To quantify the average effect over the full period, we also estimate a static version of equation (1)

$$y_{i,t} = \beta DownWind_i \times Post1988_t + \boldsymbol{X_i} \times \sum_{k=1980}^{2022} \psi_k \times \mathbf{1}(k = t) + \eta_i + \delta_t + \varepsilon_{i,t}. \quad (2)$$

When estimating equation (2), for completeness we report also the coefficients on the interaction between the total number of IDS and the post 1988 indicator. However, we remind the reader that the density of IDS close to a municipality may be correlated with unobservable municipal characteristics and, for this reason, we do not offer a causal interpretation of those coefficients.

4 Results

Figure 2 shows our main result. We estimate a positive and statistically significant relationship between wind exposure to IDS pollutants and the number of cancer deaths. The magnitude of the estimates increases over time, consistent with the observation that the emission of pollutants has continued recently and that tumors require time to develop and eventually cause death. The estimated coefficients become consistently positive since

[17] To further limit concerns with our continuous treatment variable, in Appendix E we provide evidence that the main results hold when using binary treatment indicators such as being exposed through wind to at least one IDS or being exposed through wind to a number of IDS higher than that of the median municipality.

Table 1: Wind Exposure to Land of Fires Pollutants and Cancer Deaths

	(1)	(2)	(3)	(4)	(5)
	Number of cancer deaths (all tumors)				
DownWind × Post	1.484*	1.545*	0.862**	0.926**	0.870**
	(0.831)	(0.820)	(0.389)	(0.391)	(0.368)
Total number of IDS × Post	0.643***	0.467***	0.0567	0.0666	0.0229
	(0.0785)	(0.0723)	(0.0456)	(0.0443)	(0.0510)
Municipality FE	✓	✓	✓	✓	✓
Year FE	✓	✓	✓	✓	✓
Year FE × Surface	✓	✓	✓	✓	✓
Year FE × Geographical characteristics		✓	✓	✓	✓
Year FE × Census population (1981)			✓	✓	✓
Year FE × Province FE				✓	✓
Year FE × Organized crime controls					✓
Observations	23294	23294	23294	23294	23294
Dep var mean	15.70	15.70	15.70	15.70	15.70
R-squared	0.913	0.924	0.956	0.957	0.958
F-stat	5.081	4.536	87.89	169.3	1664.5

Notes: Column (1) presents a baseline model with municipality and year fixed effects to account for time-invariant unobserved heterogeneity at the local level and common time shocks, while controlling for the total number of IDS. It also includes municipality surface (interacted with year dummies). Columns (2)-(5) progressively introduce controls fully interacted with year dummies. Column (2) includes minimum altitude as well as historical wind speed and rainfall (2001-2009). Column (3) adds census population at baseline (1981). Column (4) includes province fixed effects. Column (5) further adds organized crime controls (number of civilians killed by the Mafia and a dummy equal to 1 if the municipality was dissolved for Mafia infiltration). Heteroskedasticity and cluster-robust standard errors at the municipality level are in parentheses. Stars indicate significance levels (* $p < 0.1$, ** $p < 0.05$, *** $p < 0.01$).

the year 2000, after a prolonged latency which is consistent with the amount of time that cancerous diseases require to develop upon a prolonged exposure to pollution and to eventually cause the patient's death. Starting from 2006 onward, we estimate an average effect of roughly 2 deaths per treated municipality. Figure 2 also documents absence of pre-1988 statistically significant coefficient and no visible pre-trends. In Table 1, we show estimates of equation (2) with various sets of control variables. Across the specifications, the coefficient on $DownWind_i \times Post_t$ is consistently significant at least at the 10 percent level. Since our main dependent variable is mechanically correlated with the municipal population, it is essential to establish that our results do not depend on differential trends across municipalities of different population size. In column 3, we establish that adding population control reduces the magnitude of the estimates whilst increasing the precision of the estimates.

Effect by distance between municipality and IDS. As discussed in Section 3, our baseline estimates are based on IDS located within a distance of at most 3 kilometers from the municipality. Of those IDS, we then identify the fraction of IDS relative to which the municipality is located downwind. However, it is reasonable to expect the distance

Figure 3: Effect by distance between municipality and IDS

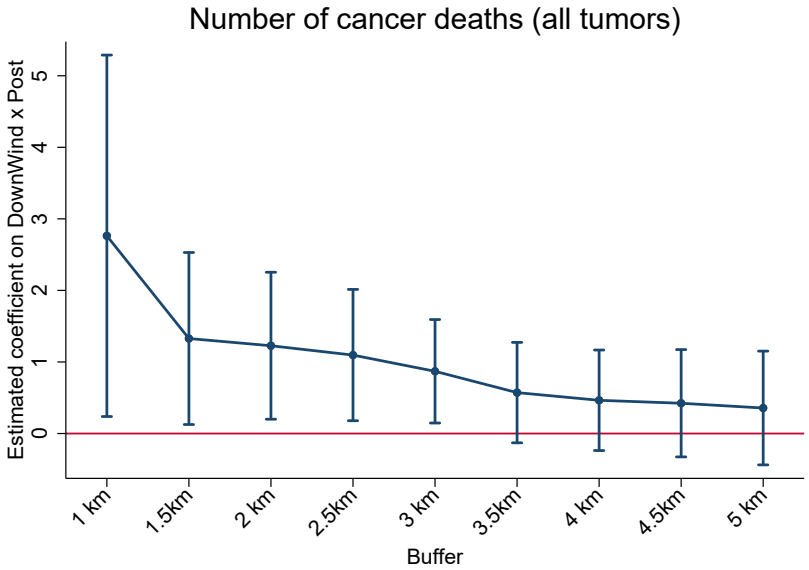

Notes: This figure reports the DownWind × Post coefficient obtained estimating equation (2). In each iteration, we reconstruct our DownWind variable and recalculate the total number of IDS close to each municipality by varying the buffer radius between the IDS center and exposed municipalities utilized to consider a municipality as being sufficiently close to an IDS (see Section 3 for details about the procedure). A buffer radius of 3 kilometers corresponds to our main specification. 95% confidence intervals are based on standard errors robust to clustering at the municipality level.

between the IDS and the municipality to be an essential predictor of exposure to pollutants stemming from the same IDS and, in turn, of the risks associated with an exposure induced by wind trajectories. In Figure 3, we replicate our results by constructing our empirical strategy on the basis of alternative fixed-radius circular buffers to whether an IDS is sufficiently close to a municipality. The results document that the effect of wind exposure decays relatively rapidly upon extending the buffer. Conversely, for small distances – smaller than our baseline – we estimate stronger effects. These results suggest that wind trajectories expose individuals to pollutants that originate from nearby IDS.

Effect by cancer type. In Panel (a) of Figure 4, we show the results obtained upon refining our dependent variable to measure the number of cancer deaths per each type of tumor. In order to ensure that the estimates are comparable across types of cancer, we standardize all dependent variables to have mean 0 and standard deviation 1. We estimate that the overall effect of exposure to toxic waste on cancer deaths is statistically significant among respiratory, bone, skin, and breast cancers. These effects are consistent with the medical literature that associates prolonged exposure to dioxin with incidence of specific types of cancer.[18] Conversely, we do not estimate statistically significant effects

[18] Fingerhut et al. (1991) document an association between dioxin exposure and respiratory cancers among highly exposed workers. See, e.g., Praud et al. (2025); Rhee et al. (2023); VoPham et al. (2020) for evidence of a link between dioxin exposure and breast cancer. Xu et al. (2016) and Kogevinas et al.

on other types of cancers. However, the observation that also among these latter types of cancers the point estimate is positive – and not significantly smaller than the coefficient that we estimate on other types of cancer – suggests that the effect of pollution exposure on cancer deaths may spill over to other types of cancer that are not necessarily directly affected by exposure to dioxin, for example because of limited capacity of the health care system at a very granular level.[19]

Youth mortality. Existing literature documents that fragile demographic groups in a society may be especially harmed by toxic pollution and that the negative effects of pollution on such fragile groups may extend beyond cancerous diseases. Specifically, children's health has been found to be particularly affected by pollutants (Chay and Greenstone, 2003; Currie and Neidell, 2005; Currie et al., 2009; Klauber et al., 2024) through asthma and other respiratory diseases. In Panel (b) of Figure 4, we focus on the effect of wind exposure to IDS on the number of deaths among individuals under 20. To this end, we utilize administrative registry data published by ISTAT which reports the count of deaths by age group, aggregated across all causes of death.[20] To ensure comparability of the estimates, we standardize all dependent variables to have mean 0 and standard deviation 1.

We estimate a positive and statistically significant effect of wind exposure on the number of deaths of individuals aged 10-19 and a comparable effect, albeit less precisely estimated, on children younger than 10. The overall effect on all individuals younger than 20 is positive and statistically significant at conventional levels.[21] In Figure A4 in the Appendix, we compare the number of deaths among individuals under 20 with other age groups. The estimates for individuals aged 01-19 are larger in magnitude than the coefficients estimated on older individuals, despite cancer being a more predominant cause of death for individuals aged 40-79.[22] This evidence suggests that individuals under 20 are disproportionally affected by the illegal disposal of toxic waste and that the negative health consequences for this fragile demographic group may go beyond the increase in the incidence of cancer.

(1997) provide evidence of an effect of dioxin exposure on cancer mortality.

[19] For example, congestion of local health facilities may induce a spillover to other forms of cancer because it limits the availability of prevention, diagnostics, surgery, and therapy facilities.

[20] Notice that these data do not allow us to separately identify specific causes of death.

[21] Conversely, we cannot estimate any statistically significant effect on young adults aged 20-29. For this group, the most common cause of death in Italy refers to external factors such as violent death or accidents.

[22] Figure A5 in the Appendix shows the share of deaths caused by cancer for each age group across Campania. The figure documents that approximately thirty percent of deceased individuals aged 0-9 and twenty percent of individuals aged 10-19 die because of cancer. Conversely, the share of cancer deaths exceeds 40 percent among individuals aged 40-69.

Figure 4: Effects by cancer type and age group

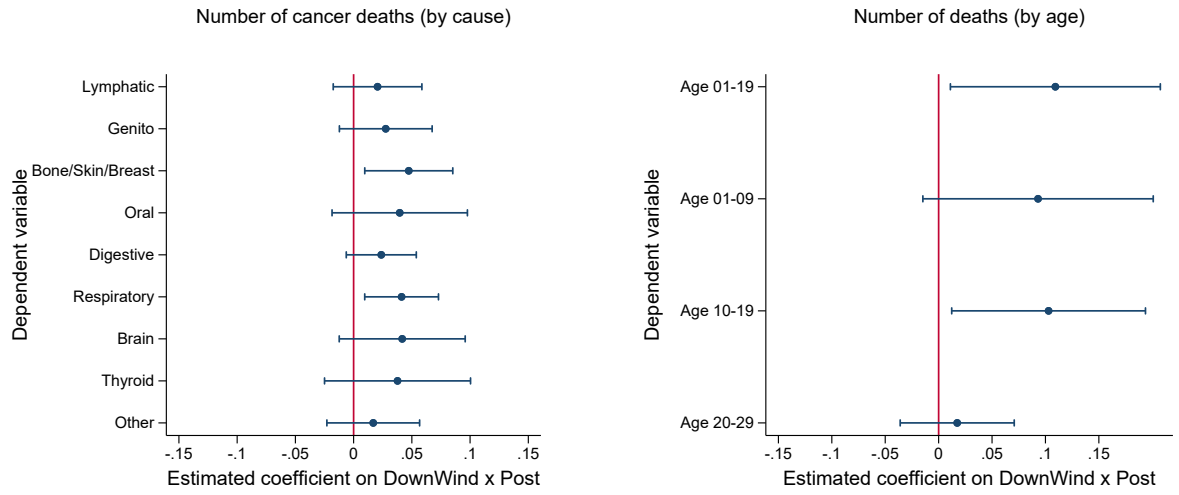

(a) Type of cancer

(b) Young cohorts, all causes of death

Notes: Panel (a) reports the DownWind × Post coefficient obtained estimating versions of equation (2) in which we refine the dependent variable so that it counts the number of cancer deaths by cancer type. The type of cancer utilized in each regression as the dependent variable is reported on the vertical axis. $N = 23,294$ in all regressions. Panel (b) reports the DownWind × Post coefficient obtained estimating versions of equation (2) in which the dependent variable counts the number of deaths by age group across any cause of death. The age group utilized in each regression as the dependent variable is reported on the vertical axis. $N = 23,294$ in all regressions. In both panels, to ensure that the estimates are comparable across specifications, we standardize all dependent variables to have mean 0 and standard deviation equal 1. 95% confidence intervals are based on standard errors robust to clustering at the municipality level.

Robustness checks. Our main estimates are robust to an extensive set of validation and sensitivity checks, reported in Appendix E for brevity. First, we cannot estimate any statistically or quantitatively meaningful effects when we use as the dependent variable the number of deaths due to causes that should be unrelated to pollution exposure (transport accidents and homicides). Second, we show that wind exposure to toxic pollutants does not affect the growth rate of population and that our results survive when adding controls for time-varying measures of the growth rate of population. Third, we show that our results hold also using binary treatment indicators such as being exposed to at least one IDS or being exposed to a number of IDS above that of the median municipality. Fourth, our estimates remain stable when changing the width of the angle that we use to consider a municipality as exposed to an IDS. Furthermore, our results are robust to varying the set of the control variables, restricting the sample to municipalities at a short distance to illegal disposal sites, as well as to weighting the regressions by each municipality's population, and estimating pseudo-Poisson maximum likelihood models.[23] Finally,

[23]Notice that the number of individuals who die because of cancer in a municipality-year is 0 in only five percent of our sample.

our estimates continue to hold when we use Conley-HAC standard errors to account for spatial correlation in the error term.

5 Concluding remarks

This paper provides systematic evidence that organized crime can cause large and persistent health externalities through its impact on the environment. We highlight social costs generated by organized crime that have not yet been credibly quantified and documented in the literature and extend our understanding of the economics of crime beyond the well-studied effects on institutions, firms, and public finances. Although our data do not allow us to measure the effect of exposure to illegal waste on cancer diagnoses, we argue that our results reflect an overall incidence of tumors because our analysis focuses on individuals that have access to the same healthcare facilities.

Our findings suggest that evaluations of organized crime that ignore health externalities substantially understate the true welfare costs of criminal activity. From a policy perspective, investments in environmental detection, cleanup, and public health surveillance in areas with a high incidence of organized crime can yield returns that are much larger—and more persistent—than those captured by traditional economic metrics alone.

Our results also speak to the broader literature on pollution and health by showing that severe and long-lasting health damage can arise outside regulated industrial activity. In contrast to conventional sources of pollution, criminally generated contaminants are deliberately concealed to remain hidden from the affected communities and regulatory bodies. As a result, their consequences on health may remain invisible for long periods as exposure continues. This feature underscores the limits of regulatory frameworks that focus exclusively on legal emissions and highlights the importance of enforcement capacity, environmental monitoring, and information disclosure in areas where criminal organizations operate.

References

Acconcia, A., G. Corsetti, and S. Simonelli (2014). Mafia and Public Spending: Evidence on the Fiscal Multiplier from a Quasi-Experiment. *American Economic Review 104*(7), 2185–2209.

Acemoglu, D., G. De Feo, and G. D. De Luca (2020). Weak States: Causes and Consequences of the Sicilian Mafia. *The Review of Economic Studies 87*(2), 537–581.

Aggeborn, L. and M. Öhman (2021). The Effects of Fluoride in Drinking Water. *Journal of Political Economy 129*(2), 465–491.

Alberti, P. et al. (2022). The "Land of Fires": Epidemiological Research and Public Health Challenges. *Heliyon 8*(12), e12331.

Alesina, A., S. Piccolo, and P. Pinotti (2019). Organized Crime, Violence, and Politics. *The Review of Economic Studies 86*(2), 457–499.

Alexander, D. and H. Schwandt (2022). The Impact of Car Pollution on Infant and Child Health: Evidence from Emissions Cheating. *The Review of Economic Studies 89*(6), 2872–2910.

Beraldo, S., M. Collaro, F. Leone, I. Marino, and D. Suppa (2026). The Mafia–Cancer Nexus: Evidence from the Land of Fires. *CSEF Working Paper No. 769*.

Bertazzi, P., D. Consonni, S. Bachetti, M. Rubagotti, A. Baccarelli, C. Zocchetti, and A. Pesatori (2001). Health Effects of Dioxin Exposure: A 20-Year Mortality Study. *American Journal of Epidemiology 153*(11), 1031–1044.

Bishop, K. C., J. D. Ketcham, and N. V. Kuminoff (2023). Hazed and Confused: The Effect of Air Pollution on Dementia. *Review of Economic Studies 90*(5), 2188–2214.

Calamunci, F. and F. Drago (2020). The Economic Impact of Organized Crime Infiltration in the Legal Economy: Evidence from the Judicial Administration of Organized Crime Firms. *Italian Economic Journal 6*(2), 275–297.

Callaway, B., A. Goodman-Bacon, and P. H. C. Sant'Anna (2024). Difference-in-Differences With a Continuous Treatment. *NBER Working Paper*, 32117.

Chay, K. Y. and M. Greenstone (2003). The Impact of Air Pollution on Infant Mortality: Evidence from Geographic Variation in Pollution Shocks Induced by a Recession. *The Quarterly Journal of Economics 118*(3), 1121–1167.

Chen, J., J. Hart, T. VoPham, E. Elliott, R. Jones, M. Ward, F. Laden, and B. Birmann (2025). Ambient Dioxin Exposure and Incidence of Lymphoid Malignancies in Large Prospective US Cohorts of Female Nurses. *Journal of Hazardous Materials 495*, 139115.

Conley, T. G. (1999). GMM Estimation with Cross Sectional Dependence. *Journal of Econometrics 92*(1), 1–45.

Currie, J. and M. Neidell (2005). Air Pollution and Infant Health: What Can We Learn from California's Recent Experience? *Quarterly Journal of Economics 120*(3), 1003–1030.

Currie, J., M. Neidell, and J. F. Schmieder (2009). Air Pollution and Infant Health: Lessons from New Jersey. *Journal of Health Economics 28*(3), 688–703.

Daniele, G. and B. Geys (2015). Organised Crime, Institutions and Political Quality: Empirical Evidence from Italian Municipalities. *The Economic Journal 125*(586), F233–F255.

Deryugina, T., G. Heutel, N. H. Miller, D. Molitor, and J. Reif (2019). The Mortality and Medical Costs of Air Pollution: Evidence from Changes in Wind Direction. *American Economic Review 109*(12), 4178–4219.

Di Cataldo, M. and N. Mastrorocco (2022). Organized Crime, Captured Politicians, and the Allocation of Public Resources. *The Journal of Law, Economics, and Organization 38*(3), 774–839.

Fenizia, A. and R. Saggio (2024). Organized Crime and Economic Growth: Evidence from Municipalities Infiltrated by the Mafia. *American Economic Review 114*(7), 2171–2200.

Fingerhut, M. A., W. E. Halperin, D. A. Marlow, L. A. Piacitelli, P. A. Honchar, M. H. Sweeney, A. L. Greife, P. A. Dill, K. Steenland, and A. J. Suruda (1991). Cancer Mortality in Workers Exposed to 2,3,7,8-Tetrachlorodibenzo-P-Dioxin. *The New England Journal of Medicine 324*(4), 212–218.

Gennaioli, C. and M. Tavoni (2016). Clean or Dirty Energy: Evidence of Corruption in the Renewable Energy Sector. *Public Choice 166*(3), 261–290.

Hollingsworth, A. and I. Rudik (2021). The Effect of Leaded Gasoline on Elderly Mortality: Evidence from Regulatory Exemptions. *American Economic Journal: Economic Policy 13*(3), 345–373.

Isen, A., M. Rossin-Slater, and W. R. Walker (2017). Every Breath You Take—Every Dollar You'll Make: The Long-Term Consequences of the Clean Air Act of 1970. *Journal of Political Economy 125*(3), 848–902.

Italian National Institute of Health (Istituto Superiore di Sanità) (2019). Report on the Health Impact in the "Land of Fires" Municipalities. Technical report, Istituto Superiore di Sanità, Rome, Italy.

Jacobsen, M. R., J. M. Sallee, J. S. Shapiro, and A. A. Van Benthem (2023). Regulating Untaxable Externalities: Are Vehicle Air Pollution Standards Effective and Efficient? *The Quarterly Journal of Economics 138*(3), 1907–1976.

Klauber, H., F. Holub, N. Koch, N. Pestel, N. Ritter, and A. Rohlf (2024). Killing Prescriptions Softly: Low Emission Zones and Child Health from Birth to School. *American Economic Journal: Economic Policy 16*(2), 220–248.

Kogevinas, M., H.Becher, T. Benn, P. Bertazzi, P. Boffetta, H. B. B. de Mesquita, D. Coggon, D. Colin, D. Flesch-Janys, M. Fingerhut, L. Green, T. Kauppinen, M. LJttorin, E. Lynge, J. D. Mathews, M. Neuberger, N. Pearce, and R. Saracci (1997). Cancer Mortality in Workers Exposed to Phenoxy Herbicides, Chlorophenols, and Dioxins. *American Journal of Epidemiology 145*(12), 1061–1075.

Le Moglie, M. and G. Sorrenti (2022). Revealing "Mafia Inc."? Financial Crisis, Organized Crime, and the Birth of New Enterprises. *Review of Economics and Statistics 104*(1), 142–156.

Marfè, G., S. Perna, and G. Mirone (2024). Hazardous Wastes in Campania (Italy) and Health Impact. *Journal of Health Science Research 9*, 13–24.

Mazza, A., P. Piscitelli, C. Neglia, G. D. Rosa, and L. Iannuzzi (2015). Illegal Dumping of Toxic Waste and Its Effect on Human Health in Campania, Italy. *International Journal of Environmental Research and Public Health 12*(6), 6818–6831.

Mirenda, L., S. Mocetti, and L. Rizzica (2022). The Economic Effects of Mafia: Firm Level Evidence. *American Economic Review 112*(8), 2748–2773.

Pinotti, P. (2015). The Economic Costs of Organised Crime: Evidence from Southern Italy. *The Economic Journal 125*(586), F203–F232.

Praud, D., A. Amadou, T. Coudon, M. Duboeuf, B. Mercoeur, E. Faure, L. Grassot, A. Danjou, P. Salizzoni, F. Couvidatf, L. Dossus, G. Severi, F. R. Mancini, and B. Fervers (2025). Association Between Chronic Long-Term Exposure to Airborne Dioxins and Breast Cancer. *International Journal of Hygiene and Environmental Health 263*, 114489.

Qiu, Y., L. Yunning, W. Shi, and M. Zhou (2024). The Impact of Ozone Pollution on Mortality: Evidence from China. *Journal of Environmental Economics and Management 125*, 102980.

Rhee, J., D. Medgyesi, J. Fisher, A. White, J. Sampson, D. Sandler, M. Ward, and R. Jones (2023). Residential Proximity to Dioxin Emissions and Risk of Breast Cancer in the Sister Study Cohort. *Environmental Research 222*, 115297.

Schlenker, W. and W. R. Walker (2016). Airports, Air Pollution, and Contemporaneous Health. *The Review of Economic Studies 83*(2), 768–809.

Slutzky, P. and S. Zeume (2024). Organized Crime and Firms: Evidence from Antimafia Enforcement Actions. *Management Science 70*(10), 6569–6596.

Sviatschi, M. M. (2022). Making a NARCO: Childhood Exposure to Illegal Labor Markets and Criminal Life Paths. *Econometrica 90*(4), 1835–1878.

VoPham, T., K. Bertrand, R. Jones, N. Deziel, N. Duprè, P. James, Y. Liu, V. Vieira, R. Tamimi, J. Hart, M. Ward, and F. Laden (2020). Dioxin Exposure and Breast Cancer Risk in a Prospective Cohort Study. *Environmental Research 186*, 109516.

Xu, J., Y. Ye, F. Huang, H. Chen, H. W. an J. Huang, J. Hu, D. Xia, and Y. Wu (2016). Association Between Dioxin and Cancer Incidence and Mortality: a Meta-Analysis. *Scientific Reports 6*, 38012.

Yang, L., Y. Lin, J. Wang, and F. Peng (2024). Achieving Air Pollution Control Targets with Technology-Aided Monitoring: Better Enforcement or Localized Efforts? *American Economic Journal: Economic Policy 16*(4), 280–315.

Zou, E. Y. (2021). Unwatched Pollution: The Effect of Intermittent Monitoring on Air Quality. *American Economic Review 111*(7), 2101–2126.

Appendix for Online Publication

A Additional Tables and Figures

Figure A1: Illegal Disposal Sites

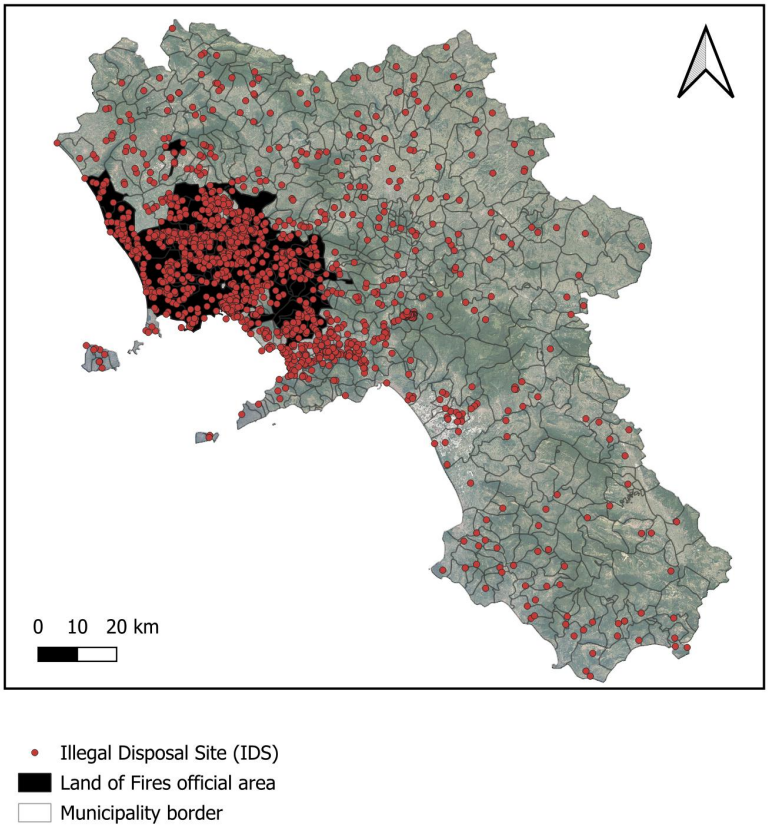

Notes: This map plots all Illegal Disposal Sites (IDS) recorded by the Campania Regional Environmental Protection Agency (ARPAC) from 2005 to 2022 (red dots). The black area marks the perimeter of the "Land of Fires", i.e., the 90 municipalities officially recognized by the Italian government as being particularly affected by the illegal disposal of toxic waste.

Table A1: Descriptive statistics I

	(1) Mean	(2) St. Dev.	(3) Min	(4) Max	(5) Obs.
Panel A) Sociodemographic characteristics					
Share of men (1991 census)	0.492	0.010	0.456	0.528	23294
Share of young pop. (1991 census)	0.283	0.049	0.145	0.418	23294
Share of elderly pop. (1991 census)	0.206	0.065	0.068	0.393	23294
Share of higher educ. (1991 census)	0.020	0.011	0.000	0.063	23294
Unemployment rate (1991 census)	0.332	0.091	0.123	0.685	23294
Employment rate agriculture (1991 census)	0.200	0.135	0.006	0.656	23294
Employment rate health (1991 census)	0.035	0.020	0.000	0.140	23294
Share of large families (1991 census)	0.182	0.064	0.043	0.367	23294
Share of foreign residents (1991 census)	0.002	0.002	0.000	0.017	23294
Avg taxable income pc (2000-2012)	6115.568	1124.536	3081.298	11469.278	23294
Panel B) Geographical characteristics					
Minimum altitude (km)	0.152	0.153	-0.002	0.829	23294
Radon 2007 (bq/m^3)	236.513	135.725	10.000	1360.200	23294
Surface (km2)	24.451	23.042	0.105	186.875	23294
$DownWind_i$	0.365	0.379	0.000	1.000	23294
Total number of IDS	5.511	8.982	0.000	55.000	23294
Panel C) Meteorological variables (2001-2009)					
Historical avg humidity (2001-2009)	74.028	1.589	67.748	78.328	23294
Historical avg temperature (2001-2009)	15.478	0.802	13.259	17.203	23294
Historical rainfall (2001-2009)	2.646	0.234	1.886	3.104	23294
Historical avg wind direction (2001-2009)	212.876	114.796	0.146	359.995	23294
Historical avg wind speed (2001-2009)	0.474	0.227	0.017	1.516	23294
Panel D) Census population (1981–2011)					
Census population (1981)	7212.328	11560.460	469.000	103605.000	23294
Census population (1991)	7801.793	12210.415	441.000	101361.000	23294
Census population (2001)	8065.481	12720.332	400.000	97999.000	23294
Census population (2011)	8270.974	12977.950	280.000	108793.000	23294
Annual population estimates	7909.690	12563.110	220.000	123758.000	23294
Panel E) Organized crime variables					
Number of civilian killed by Mafia (1967-2004)	0.203	0.803	0.000	8.000	23294
Municipality dissolved for mafia infiltration (1991-2022)	0.144	0.351	0.000	1.000	23294

Notes: See Appendix B for information about the data sources and the years in which each variable is available.

Table A2: Descriptive statistics II

	(1) Mean	(2) St. Dev.	(3) Min	(4) Max	(5) Obs.
Panel A) Malignant cancers (1980-2022)					
All malignant tumors	15.703	25.581	0.000	273.000	23294
Lymphatic cancers	1.240	2.173	0.000	22.000	23294
Genitourinary cancers	2.362	3.955	0.000	47.000	23294
Bone/Skin/Breast cancers	1.481	2.836	0.000	40.000	23294
Oral cancers	0.225	0.577	0.000	8.000	23294
Digestive cancers	5.161	8.541	0.000	94.000	23294
Respiratory cancers	3.701	6.628	0.000	74.000	23294
Brain/eyes cancers	0.390	0.875	0.000	10.000	23294
Thyroid cancers	0.084	0.315	0.000	5.000	23294
Other cancers	1.059	2.047	0.000	26.000	23294
Panel B) All-cause deaths by age group (1980-2022)					
Age 01-19	0.492	1.513	0.000	93.000	23294
Age 01-09	0.184	0.746	0.000	46.000	23294
Age 10-19	0.308	0.932	0.000	51.000	23294
Age 20-29	0.573	1.306	0.000	26.000	23294
Age 30-39	0.855	1.807	0.000	44.000	23294
Age 40-49	1.954	3.595	0.000	43.000	23294
Age 50-59	4.685	8.098	0.000	85.000	23294
Age 60-69	9.660	15.960	0.000	167.000	23294
Age 70-79	17.442	26.491	0.000	265.000	23294
Age 80-89	20.777	29.763	0.000	342.000	23294
Age 90+	7.672	11.857	0.000	181.000	23294
Panel C) Placebos (1980-2022)					
Sexually transmitted diseases	0.002	0.040	0.000	1.000	23294
Appendicitides	0.008	0.093	0.000	2.000	23294
Eye diseases	0.003	0.059	0.000	2.000	23294
Venous disorders	0.085	0.322	0.000	4.000	23294
Chronic heart diseases	0.212	0.555	0.000	9.000	23294
Ischemic heart diseases	8.274	12.904	0.000	148.000	23294
Benign cancers	0.063	0.276	0.000	6.000	23294
Strokes	8.681	11.829	0.000	121.000	23294
Mental disorders	0.737	1.806	0.000	29.000	23294
Homicides	0.135	0.595	0.000	14.000	23294
Transport accidents	0.520	1.136	0.000	30.000	23294

Notes: See Appendix B for information about the data sources and the years in which each variable is available.

Figure A2: IDS and municipalities

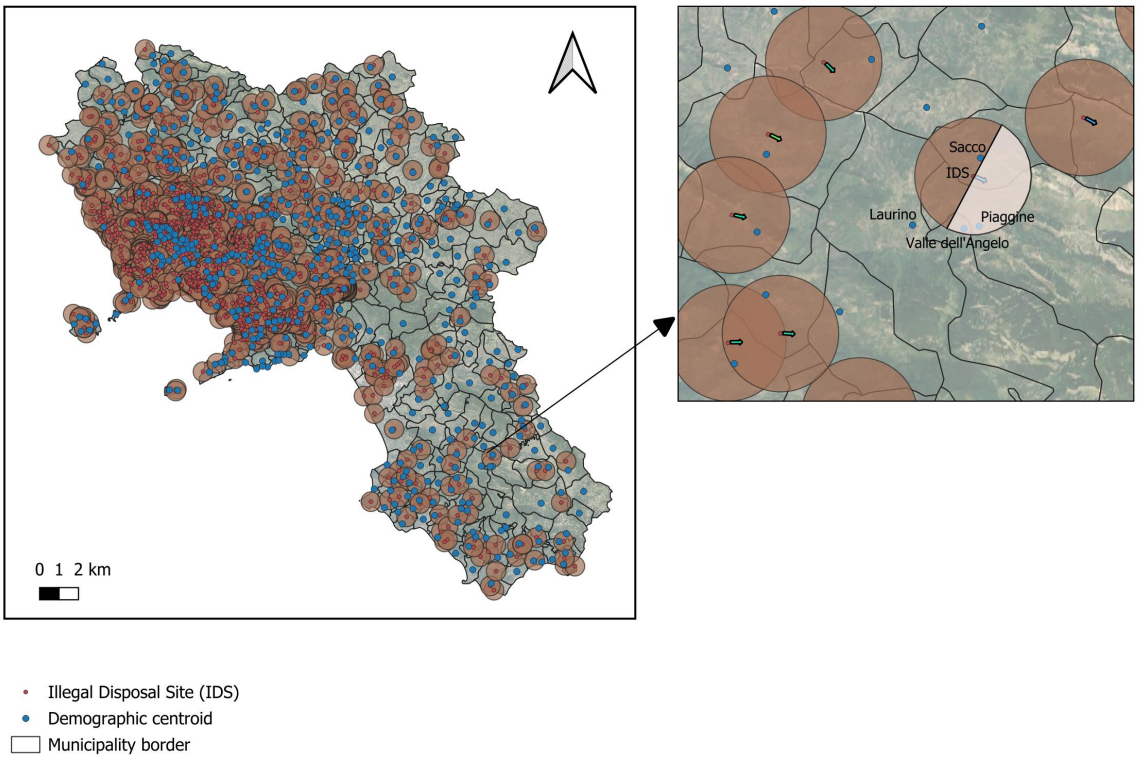

Notes: This figure displays the spatial buffer used to identify treated units. Each circle represents a 3 km radius centered on each Illegal Disposal Site (IDS), marked by red dots. Blue dots represent the demographic centroids of municipalities, defined in Appendix D. A municipality is classified as affected by the buffer if any part of its demographic centroid intersects the 3 km buffer circle. To define downwind exposure, this buffer-based classification is combined with the historical average wind direction at each IDS, denoted by $\overline{WINDDIR_s}$. The top-right panel provides a zoomed-in view where a single IDS intersects multiple municipalities (Sacco, Piaggine, and Valle dell'Angelo). Based on $\overline{WINDDIR_s}$, Piaggine and Valle dell'Angelo fall within the wind exposed region (shaded area).

Figure A3: Balance test

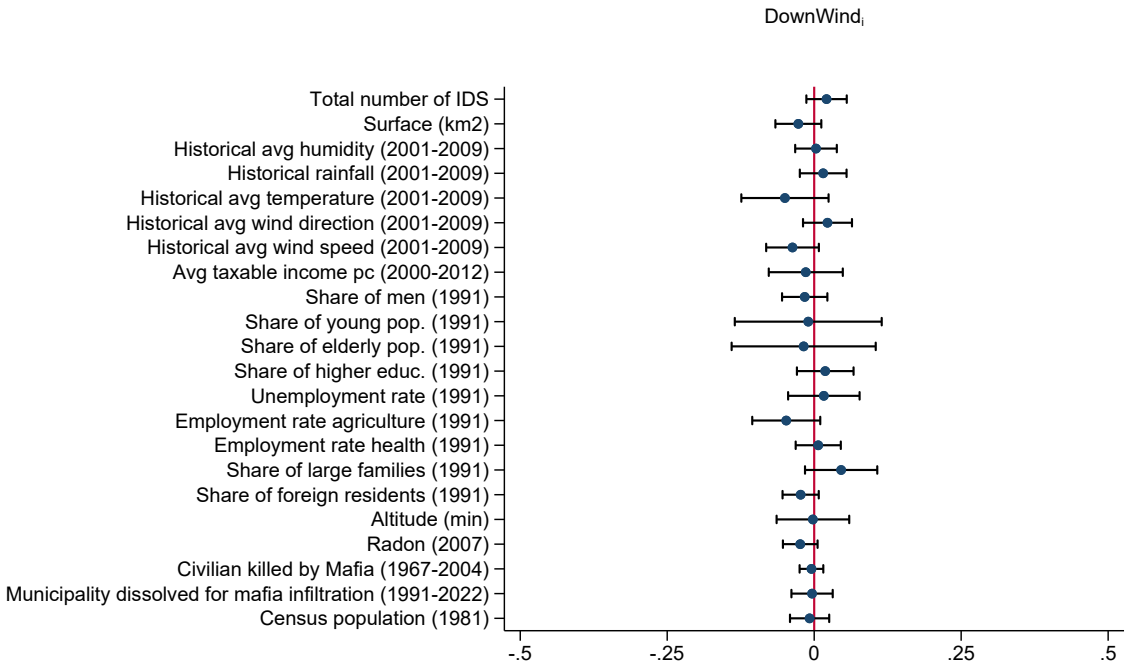

Notes: This figure reports OLS estimates obtained from regressing the variable $DownWind_i$ on the control variables specified on the vertical axis as well as province fixed effects. All covariates have been standardized to have mean zero and unit standard deviation. 95% confidence intervals are based on standard errors robust to heteroskedasticity.

Figure A4: Effects by age group, all causes of death

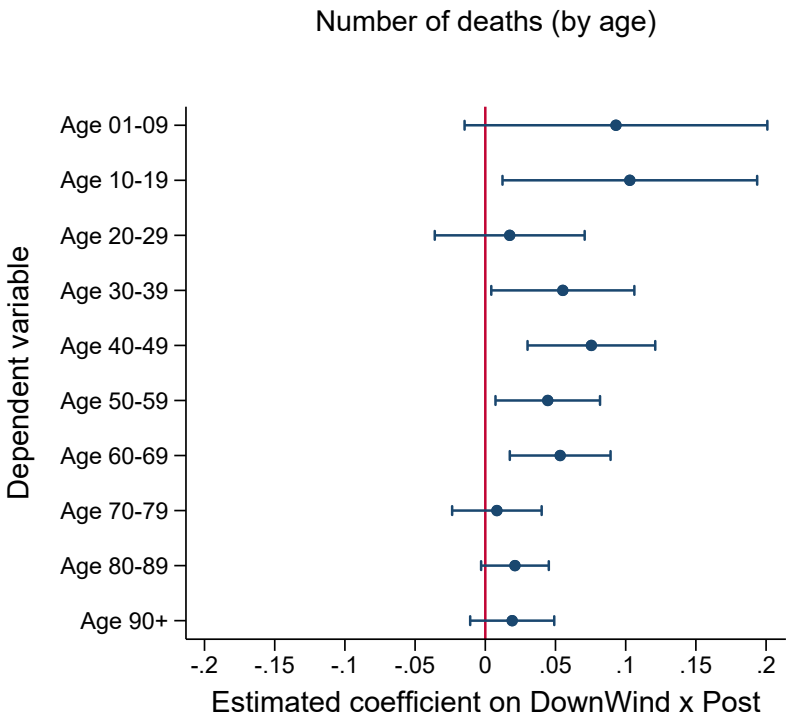

Notes: The figure reports the DownWind × Post coefficient obtained estimating versions of equation (2) in which the dependent variable counts the number of deaths by age group across any cause of death. The age group utilized in each regression as the dependent variable is reported on the vertical axis. $N = 23,294$ in all regressions. To ensure that the estimates are comparable across specifications, we standardize all dependent variables to have mean 0 and standard deviation equal 1. 95% confidence intervals are based on standard errors robust to clustering at the municipality level.

Figure A5: Share of cancer deaths by age group in Campania, 2003–2022

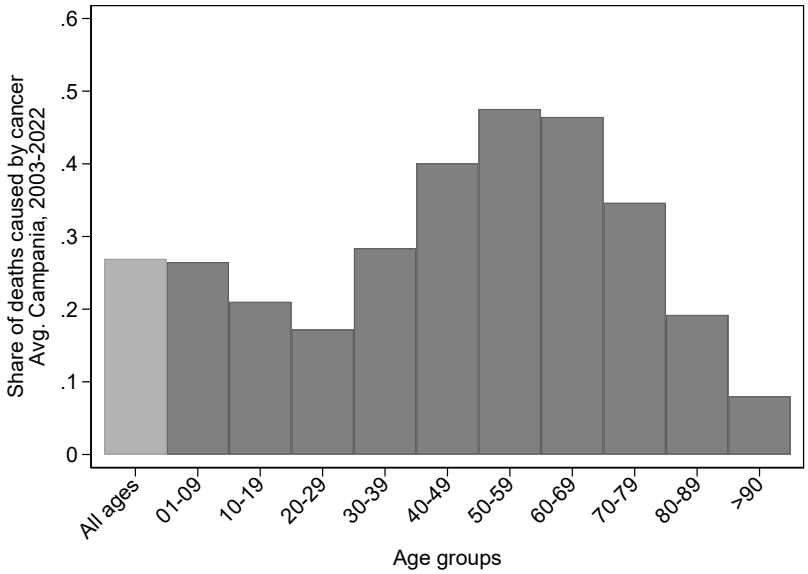

Notes: The figure reports the distribution of the share of deaths caused by cancer (as a fraction of the total number of deaths) by age groups across Campania, averaging over the whole period for which the data are available (2003–2022) with the exclusion of 2020. The lighter bar reports the overall share across all age groups.

B List of data sources

Illegal Disposal Sites (IDS). We retrieve data on Potentially Contaminated Sites (henceforth, PCS) from the Agency for the Protection of the Environment (ARPAC) of the Campania region. The sites are labeled as "potentially" contaminated because no systematic environmental assessment has been carried out at each location. The PCS inventory provides, for each site, information about the type of pollutant, a brief description of the activity at the location, and its exact geographic coordinates. Since the inventory also includes sites contaminated for reasons unrelated to the illegal toxic-waste network (e.g., mismanagement of regular municipal waste), we exploit specific descriptions to identify Illegal Disposal Sites (henceforth, IDS) within the full set of PCS. IDS are those sites directly associated with the Land of Fires system of illegal waste disposal. Specifically, we classify as IDS all sites whose descriptions include the following terms: abandoned waste on land, waste dumping in aquatic areas, uncontrolled waste abandonment, abandoned area, dioxin-contaminated area, toxic waste, dismissed industrial area, dismissed gas station, natural lake area, eco-bales, temporary waste storage site, unauthorized landfill, contaminated public area, uncontrolled landfill, hydrocarbon storage, major accident hazard industrial facility, storage of hazardous toxic waste, public park, and quarry.[24] We, instead, exclude all sites explicitly categorized as "business", "industrial", "gas station", or "hotel".

Historical wind trajectories. We measure historical wind trajectories using daily data covering the period 2001–2009 from 47 meteorological stations located across 45 municipalities in Campania.[25] We obtain these data from the regional agrometeorological archive of the Campania Department of Agriculture.[26] For each station, we also collect information on wind speed, temperature, humidity, and rainfall.

Causes of death data. We utilize data for the period 1980–2022 from the Italian Institute of Statistics (ISTAT) on deceased individuals by their municipality of residence and the cause of death according to the International Classification of Diseases (ICD). Due to privacy concerns, ISTAT data report the exact number of deceased individual per each cause only when at least three individuals of the same gender die in a municipality during a year. Thus, the data do not allow us to identify individuals deceased because of cancer in those cases, which nevertheless are negligible in the data.[27] We impute 0 cancer deaths in these cases.

[24] Anecdotal evidence suggests that abandoned quarries were frequently used for illegal waste disposal once nearby locations used for open-air burning were no longer available.

[25] The database is available from 2001 onward. Hence, using earlier periods is not possible.

[26] See https://agricoltura.regione.campania.it/meteo/archivio_meteo.html.

[27] Undisclosed cause of death occurs in less than 1 percent of our sample.

Each death is classified according to the International Classification of Diseases (ICD-9 up to 2003, ICD-10 from 2003 onwards in the ISTAT dataset): lymphatic and hemopoietic tissue cancers (2000-2089 and C81-C96), genitourinary cancers (1790-1899 and C51-C58, C60-C63, C64-C68), bone, connective tissue, skin, breast cancers (1700-1769 and C40-C41, C43-C49, C50), lips, oral cavity, pharynx (1400–1499 and C00–C14), digestive system and peritoneum cancers (1500-1599 and C15-C26), respiratory system and intrathoracic organs tumors (1600-1659 and C30-C39), eyes and brain cancers (1900-1909, 1910-1929 and C69, C70-C72), thyroid cancers (1930-1949 and C73-C75), as well as other residual categories such as tumors of unspecified nature, carcinoma, multiple cancers, tumors of uncertain behaviour (1950-1999, 2300-2349, 2390-2399, 2350-2389 and C76-C80, C97, D00-D09, D37-D48).

Data on death by age group. We utilize data for the period 1980–2022 from the Italian Institute of Statistics (ISTAT) on deceased individuals by their municipality of residence and age group (five-year bins). Due to privacy concerns, ISTAT data report the exact number of deceased individual per each age group only when at least three individuals of the same gender die in a municipality during a year. Thus, the data do not allow us to identify the age of individuals deceased in those cases, which nevertheless are negligible in the data.[28] We impute 0 deaths across all age groups in these cases.

Data on death by cause of death and age group. We utilize data for the period 2003–2022 from the Italian Institute of Statistics (ISTAT) on deceased individuals by their province of residence, age group (five-year bins), and cause of death.

Each death is classified according to the International Classification of Diseases (ICD-9 up to 2003, ICD-10 from 2003 onwards in the ISTAT dataset): lymphatic and hemopoietic tissue cancers (2000-2089 and C81-C96), genitourinary cancers (1790-1899 and C51-C58, C60-C63, C64-C68), bone, connective tissue, skin, breast cancers (1700-1769 and C40-C41, C43-C49, C50), lips, oral cavity, pharynx (1400–1499 and C00–C14), digestive system and peritoneum cancers (1500-1599 and C15-C26), respiratory system and intrathoracic organs tumors (1600-1659 and C30-C39), eyes and brain cancers (1900-1909, 1910-1929 and C69, C70-C72), thyroid cancers (1930-1949 and C73-C75), as well as other residual categories such as tumors of unspecified nature, carcinoma, multiple cancers, tumors of uncertain behaviour (1950-1999, 2300-2349, 2390-2399, 2350-2389 and C76-C80, C97, D00-D09, D37-D48).

Other data sources. We collect municipal-level variables from several sources. We obtain demographic and socio-economic variables from the 1991 population census conducted by ISTAT (Italian National Institute of Statistics), including the shares of men,

[28] Undisclosed age of death occurs in less than 1 percent of our sample.

young population (aged 19 or below), elderly population (aged 60 or above), residents with tertiary education, unemployment, employment in the agriculture and health sectors, large families (five or more components), and foreign residents. We also exploit the Italian National Institute of Statistics to retrieve geographic information on municipality's surface and minimum altitude. Information on municipal taxable income over 2000–2012 comes from the Ministry of Economy and Finance. Data on radon concentrations are taken from A2C, a professional consortium specialized in radon measurement and in the remediation of contaminated sites. Population data come from ISTAT and include the decennial censuses (1981, 1991, 2001, and 2011), as well as annual population estimates. Information on the exact location of each census block in the region, used in the construction of population-weighted centroids, is drawn from the 2001 ISTAT population census. Data on dissolutions of municipality councils between 1991 and 2022 are from the non-for-profit organization WikiMafia. Finally, data on civilian victims of mafia-related violence over the years 1967–2004 are provided by *Libera*, a civil-society organization that assembles the main national database of innocent victims of organized crime.

C Wind Direction Technical Appendix

C.1 Estimation of wind direction at each IDS

This section outlines the procedure adopted to approximate historical wind direction at each of the 1,667 Illegal Disposal Sites (IDS) located in the Campania region based on records from the 47 meteorological stations located in the region and daily measures for the period 2001–2009. Figure C2 plots meteorological stations location.

First, for each IDS_s, meteorological station j, and day τ, we compute the angle between the wind direction vector ($WINDDIR_{j,\tau}$) and the vector linking the meteorological station to the IDS (the connection vector), following Qiu et al. (2024). We denote the angle between the connection vector and wind direction as $\theta_{s,j,\tau}$. Second, we define the binary indicator $WI_{s,j,\tau}$ as equal to 1 if $\theta_{s,j,\tau}$ falls within the range $[0°, 90°]$. This area represents the *acceptable* region for our purposes, as it is the half-space delimited by a line orthogonal to the wind direction vector and passing through the meteorological station j (see Figure C1). Intuitively, meteorological station j does not provide information about wind direction at IDS_s if the wind originating from j does not bear towards s.

Since wind direction is an angular variable, it cannot be averaged directly in degrees. We therefore first express each daily wind observation as two signed orthogonal components.[29] To aggregate information from *acceptable* wind stations into one single direction vector per each $s\tau$ pair, we implement a spatial matching technique inspired by the K-Nearest-Neighbors methodology. Each day, we consider as valid nearest neighbors the five nearest meteorological stations for which $WI_{s,j,\tau} = 1$ and weight wind direction in station j on day τ proportionally to the (inverse of) the distance between station j and IDS_s.[30] In this way, closer actual stations receive higher weights whereas farther actual stations receive lower weights. Stations that are either too far away – i.e., not among the five nearest neighbors – or experience wind direction that cannot predict wind direction at station s in day τ are discarded. For each selected neighboring station, the weighted orthogonal components are computed as $X^W_{s,j,\tau} = \alpha_{s,j,\tau} \times WI_{s,j,\tau} \times X_{j,\tau}$ and $Y^W_{s,j,\tau} = \alpha_{s,j,\tau} \times WI_{s,j,\tau} \times Y_{j,\tau}$. These are then aggregated across the selected stations to obtain the synthetic daily component vector. We recover wind direction as a mathematical angle from the aggregated Cartesian components using the two-argument arc-tangent, $\text{atan2}(Y, X)$, and then normalize the resulting angle to the interval $[0, 360)$. Hence, angles are measured relative to the Cartesian x-axis, rather than as meteorological azimuths

[29] For each meteorological station j and day τ, we define our project's internal coordinate system as $X_{j,\tau} = -WINDSPEED_{j,\tau} \sin(WINDDIR^{rad}_{j,\tau})$ and $Y_{j,\tau} = -WINDSPEED_{j,\tau} \cos(WINDDIR^{rad}_{j,\tau})$, where $WINDDIR^{rad}_{j,\tau}$ denotes wind direction expressed in radians.

[30] We define the inverse distance as $Dist^{inv}_{s,j} = \frac{1}{d_{s,j}}$ where $d_{s,j}$ represents the distance (in km) between IDS_s and station j. Then, we compute the total inverse distance within the five nearest neighbors as $TotDist^{inv}_{s,\tau} = \sum_{j \in \mathbf{J}_{s,\tau}} Dist^{inv}_{s,j}$, where $\mathbf{J}_{s,\tau}$ denotes the set of nearest neighbors. The weights are then defined as $\alpha_{s,j,\tau} = \frac{Dist^{inv}_{s,j}}{TotDist^{inv}_{s,\tau}}$.

measured clockwise from North. This convention is adopted consistently throughout the entire analysis. In particular, we adopt the same Cartesian convention also to compute the vector linking each meteorological station to the corresponding IDS, as well as the vector linking each IDS to the municipality falling within the buffer. The wind direction at IDS_s on day τ is therefore recovered by applying the two-argument arc-tangent to the aggregated components: $WINDDIR^{rad}_{s,\tau} = \text{atan2}\Big(\sum_{j=1}^{5} Y^W_{s,j,\tau}, \sum_{j=1}^{5} X^W_{s,j,\tau}\Big)$. We then convert the resulting angle into degrees: $WINDDIR_{s,\tau} = WINDDIR^{rad}_{s,\tau} \cdot \frac{180}{\pi}$. Hence, the wind direction at IDS_s on day τ ($WINDDIR_{s,\tau}$) is obtained from the weighted orthogonal components of the selected stations:

$$WINDDIR_{s,\tau} = \text{atan2}\left(\sum_{j=1}^{5} Y^W_{s,j,\tau}, \sum_{j=1}^{5} X^W_{s,j,\tau}\right) \cdot \frac{180}{\pi}.$$

Finally, we compute the historical average wind direction at each IDS ($\overline{WINDDIR_s}$) over the entire period 2001-2009. Figure C3 reports the estimated directions at each IDS.

C.2 Historical wind direction cross validation

In this section, we establish that $\overline{WINDDIR_s}$ captures persistent atmospheric circulation patterns that are relevant for our entire observation period, 1980–2022, even though we can construct the measure only using observed wind patterns over the period 2001–2009. To this end, we compare our historical wind-direction measure at each IDS, estimated based on observed wind patterns at 47 meteorological stations, with the Copernicus Climate Data Store's UERRA regional reanalysis for Europe on single levels, from which we retrieve daily wind-direction data at 10 meters above ground for 1980–2019 over the Campania region.

We first identify all UERRA grid cells intersecting Campania, which yields 173 cells in total (11 km $\times$ 11 km resolution). To ensure full comparability with our main measure, we compute for each cell the long-run prevailing wind direction over 1980–2019 using a circular mean defined under the same angular convention adopted in the previous subsection. We then assign each Illegal Disposal Site (IDS) to the UERRA grid cell in which the IDS is located and attach the corresponding grid-level prevailing wind direction.[31]

We assess the correlation between $\overline{WINDDIR_s}$ and $\overline{WINDDIR_s}^{UERRA}$ estimating the following equation:

[31] Since UERRA cells are identified by the coordinates of their centroids, we assign each IDS to the geographically nearest grid-cell centroid. Among the 173 cells intersecting Campania, 124 are matched to at least one IDS after this procedure.

$$\overline{WINDDIR_s} = \alpha + \beta \overline{WINDDIR_s}^{UERRA} + \varepsilon_s. \tag{3}$$

where $\overline{WINDDIR_s}^{UERRA}$ is the Copernicus-based prevailing wind direction over 1980–2019 at each IDS s and ε_s is the error term.

Figure C4 shows that our main measure of wind direction at each IDS is positively correlated with the UERRA-based prevailing wind direction for IDS that are sufficiently close to the centroid of the UERRA cell. The relationship is strongest when the cell lies geographically close to the site, and it weakens as the site-to-grid distance increases. This pattern is consistent with attenuation arising from spatial mismatch and provides reassurance that our measure is not merely capturing transitory or idiosyncratic weather conditions, but instead constitutes an informative proxy for historical wind direction.[32]

The validation exercise presented in Figure C4 confirms that wind patterns reconstructed over 2001–2009 are informative about historically prevalent trajectories over the full period of our analysis. Yet, one may still be concerned that $\overline{WINDDIR_s}^{UERRA}$ is a more reliable measure than $\overline{WINDDIR_s}$. Indeed, $\overline{WINDDIR_s}^{UERRA}$ approximates wind trajectories based on 173 locations, as opposed to the 47 stations that we use to construct $\overline{WINDDIR_s}$, over a time span that more closely matches the window of our empirical analysis.

In Figure C5, we provide evidence that our measure leverages significantly more granular variation than the UERRA data. Indeed, although 173 UERRA cells overlap, at least in part, with the Campania region, each cell's information is based on the estimation of a wind model based on long-distance patterns rather than on actual observational data. In Figure C5, we show the pairwise correlation between the actual wind direction observed at each of the 47 meteorological stations in the Campania region and the wind patterns estimated by UERRA in the cell to which each meteorological station belongs.[33] The figure shows no evidence of a meaningful correlation, suggesting that UERRA estimates cannot approximate precisely the wind patterns that are observed at each meteorological station. More broadly, the evidence reported in Figure C5 indicates that international wind pattern repositories offer a noisy estimate of actual wind patterns at the granular level that our analysis requires. Based on this evidence, we conclude that we can approximate wind patterns at each IDS more precisely by relying on observed wind trajectories

[32] Figure C4 offers a descriptive comparison between the ARPAC-based and UERRA-based prevailing wind directions in raw degree space. Because wind direction is a circular variable, this exercise should not be interpreted as a formal test of angular equivalence. Nevertheless, our identification strategy does not depend on the exact wind angle itself, but on whether IDS are classified as upwind or downwind relative to each municipality. Accordingly, Table C1 reports a complementary validation exercise in which we compare the municipality-level share of upwind IDS based on the UERRA historical wind direction with the corresponding share used in the main analysis.

[33] To estimate this correlation, we rely on the period 2001–2009 also for UERRA data.

at the 47 meteorological stations of the Campania ARPAC regional authority although such data are only available since 2001.

Figure C1: Wind influence dummy ($WI_{s,j,\tau}$)

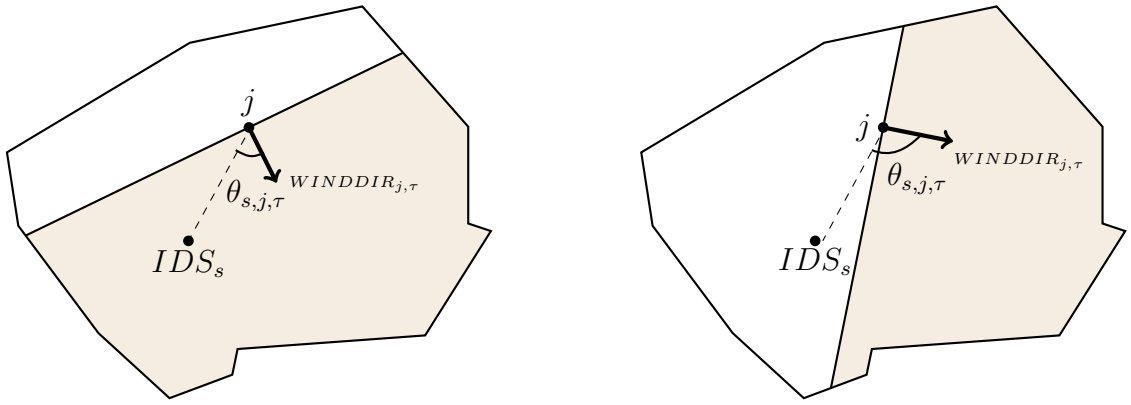

(a) $WI_{s,j,\tau} = 1$ (b) $WI_{s,j,\tau} = 0$

Notes: Panel (a) shows an example in which $WI_{s,j,\tau} = 1$ since the angle between the connection vector (dashed line from station j to IDS_s) and the wind direction vector falls within $[0°, 90°]$. Panel (b) shows an example in which $WI_{s,j,\tau} = 0$. The wind exposed region is defined by the half-space delimited by a line orthogonal to the wind direction vector and passing through the meteorological station j.

Figure C2: Meteorological stations distribution map

Notes: This map shows the geographic distribution of the 47 meteorological stations used to measure the weather variables employed in the empirical analysis.

Figure C3: Historical average wind direction at each IDS

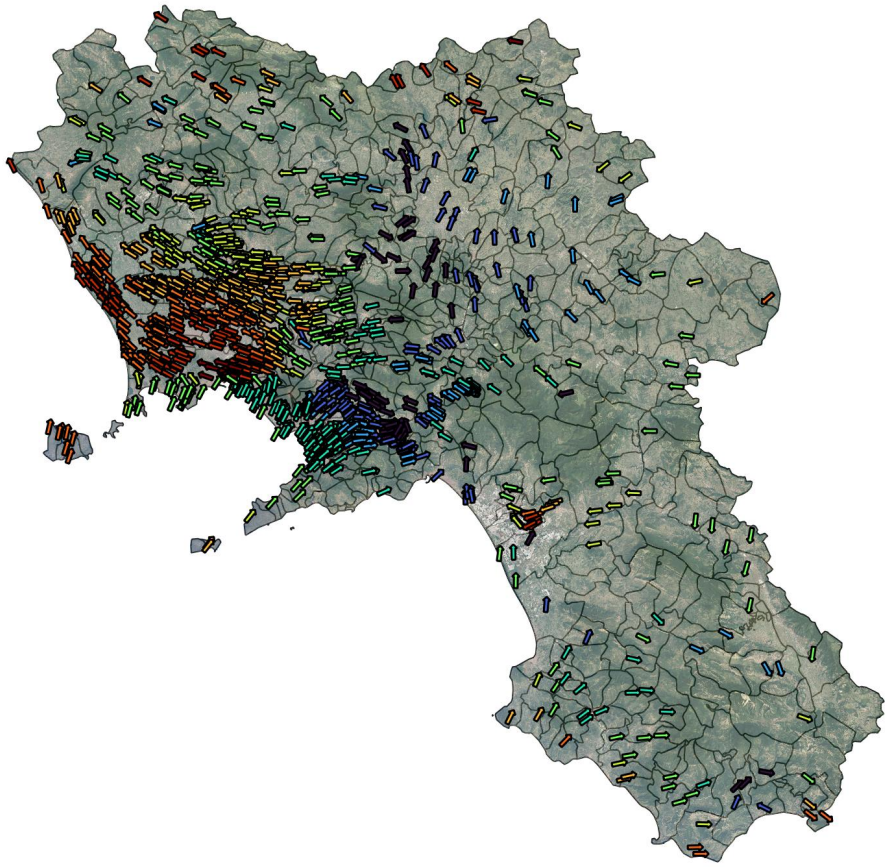

Notes: This figure displays the estimated historical average wind direction (2001-2009) at each of the the 1,667 IDS. Color intensity denotes wind speed (darker red arrows correspond to higher average wind speeds).

Figure C4: Correlation between $\overline{WINDDIR_s}$ and $\overline{WINDDIR_s}^{UERRA}$

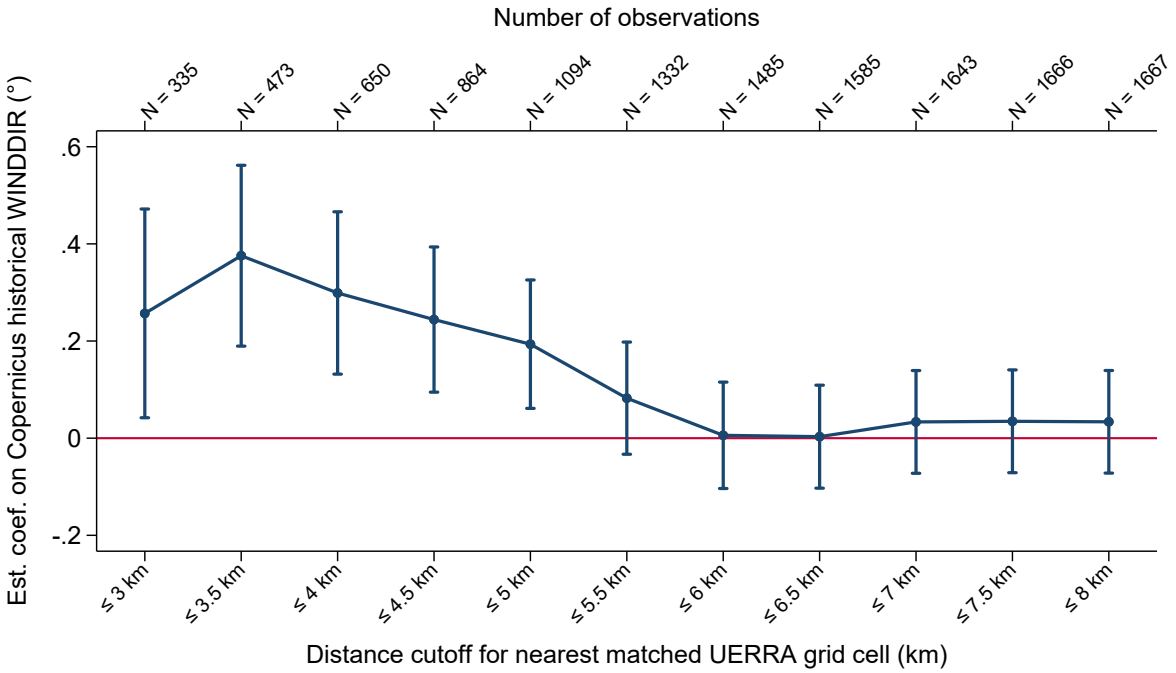

Notes: The figure plots the estimated coefficient on the Copernicus/UERRA historical prevailing wind direction from equation (3). Each point corresponds to a separate regression in which the sample is restricted to IDS whose distance to the matched UERRA grid cell centroid does not exceed the threshold reported on the horizontal axis. 95% confidence intervals are based on standard errors robust to heteroskedasticity. The labels above the plot report the number of IDS included in each regression.

Figure C5: Correlation between meteorological stations and UERRA estimates

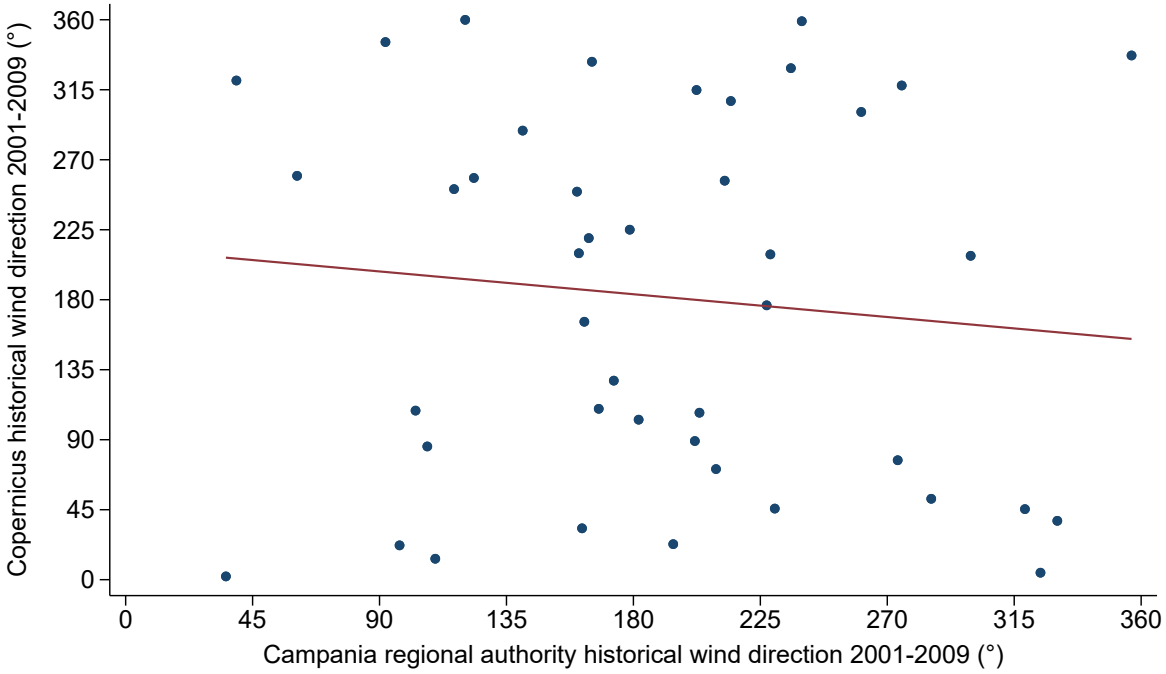

Notes: The figure plots the historical average wind direction at each of the 47 meteorological stations in Campania over 2001–2009 against the corresponding UERRA-based prevailing wind direction pattern over the same period. Each station is matched to the UERRA grid to which the station belongs. The solid line shows the linear fit.

Table C1: Cross-validation of downwind classification

	(1)	(2)	(3)	(4)
	DownWind			
DownWind (Uerra)	0.287***	0.278***	0.273***	0.261***
	(0.0448)	(0.0450)	(0.0459)	(0.0468)
Surface		✓	✓	✓
Minimum altitude			✓	✓
Province FE				✓
Observations	542	542	542	542
Dep var mean	0.365	0.365	0.365	0.365
R-squared	0.0885	0.107	0.108	0.119
F-stat	41.03	30.79	20.90	12.61

Notes: The dependent variable is the municipality-level share of upwind IDS adopted in the main analysis. The main explanatory variable is the corresponding municipality-level share computed using the UERRA-based prevailing wind measure calculated using data spanning the period 1980-2019. Column (1) reports the pairwise correlation between the two variables. Column (2) adds municipality surface, whereas column (3) includes minimum altitude. Column (4) further adds province fixed effects. Standard erorrs robust to heteroskedasticity are reported in parentheses. Stars indicate significance levels (* $p < 0.1$, ** $p < 0.05$, *** $p < 0.01$).

D Calculation of population-weighted municipality "demographic" centroids

To identify wind trajectories between the contaminated site and individuals that are exposed to pollutants, it is essential to geo-locate each municipality taking into account that the urban center may not necessarily be the geographical center (i.e., the centroid) of the municipality. We utilize population data and the exact location of each census block of the Campania region (approximately 20,000 census blocks, equivalent to an average of circa 40 census blocks per municipality) as of the 2001 population census. Then, we define the "demographic" centroid of each municipality i – which we use as our proxy for the geo-location of individuals that live in the municipality – as the weighted average of all the geometric centroids of each municipality's census blocks $b(i)$, where the weight on each block's centroid depends on the share of the municipality's population that lives in that block, $\frac{Pop_{b(i)}}{Pop_i}$.[34]

Intuitively, if all individuals who live in a municipality are concentrated within one census block, what really matters for assessing their exposure to IDS is the position of that census block rather than the position of the geographical centroid of the municipality. Formally, we define the coordinates of the "demographic" centroid (x_i, y_i) as $x_i = \sum_{b=1}^{B} \left(\frac{Pop_{b(i)}}{Pop_i} \times x_{b(i)} \right)$ and $y_i = \sum_{b=1}^{B} \left(\frac{Pop_{b(i)}}{Pop_i} \times y_{b(i)} \right)$, where the pair $(x_{b(i)}, y_{b(i)})$ identifies the coordinates of the geographical centroid of census block b. Figure D1 clarifies why identifying the "demographic" centroid is essential for our purposes. The geographic centroid would not yield an accurate representation of where people live in this municipality while the "demographic" centroid offers a more accurate proxy.

[34] Notice that census blocks are nested into municipalities.

Figure D1: Example of "demographic" centroid

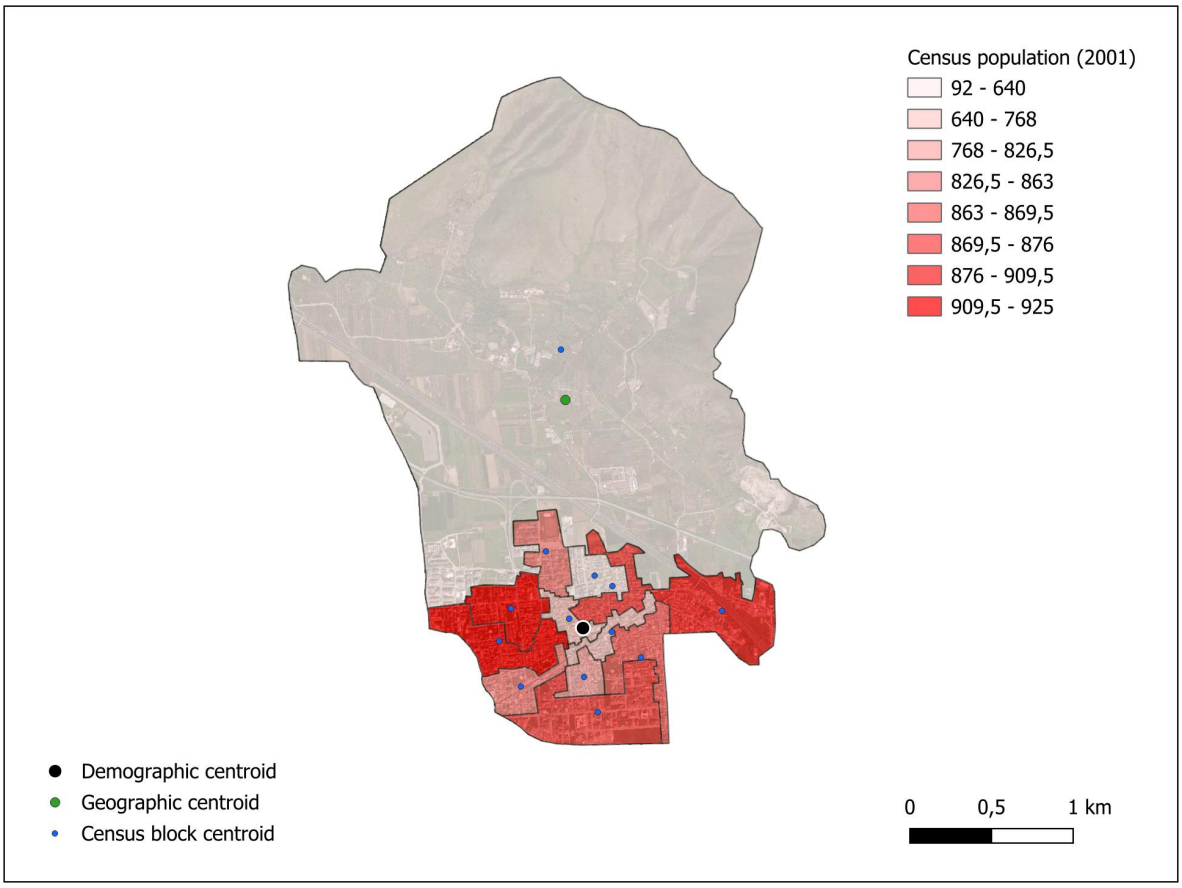

Notes: This figure displays the "demographic" and geographical centroids for the municipality of San Prisco (province of Caserta), which consists of 13 census blocks. Shaded polygons represent census blocks, with darker tones denoting higher 2001 census population. Blue dots mark the geographic centroids of each census block. The green dot is the municipality's geographic centroid, whereas the black dot is the demographic centroid. The latter is computed as the population–weighted average of census block centroids using 2001 census data. Since wind exposure is measured over 2001–2009, the 2001 census provides the closest snapshot of the spatial distribution of residents in this period. The underlying satellite image shows that the northern part of San Prisco is largely uninhabited, while residential areas are concentrated in the south. Consistently, the demographic centroid lies in the populated southern area rather than at the geometric center of the municipality, making it a more suitable proxy for individual exposure to pollution.

E Robustness checks

We conduct a battery of robustness checks to assess the validity of our Difference-in-Differences estimates.

No effect on the number of deaths due to other diseases. We assess that our results do not reflect general changes in the overall mortality across municipalities by looking at the number of individuals died because of causes of death that are unlikely to be affected by pollution from the Land of Fires. Figure E1 reports event-study estimates for a set of non-cancer outcomes (sexually transmitted diseases, appendicitis, eye diseases, venous diseases, chronic and ischemic heart diseases, benign tumors, strokes, and mental disorders), following the main specification reported in Equation 1. Across panels, estimated coefficients do not display systematic differential trends before or after 1987.

No effect on violent causes of death. In Figure E2, we focus on causes of violent death. This test is particularly important to ensure that our results are not confounded by different levels of criminal activity across municipalities. The figure reports event study coefficients for homicides and transport accidents. Estimates provide no evidence of causal effects on these outcomes, further reassuring about the validity of our research design.

Robustness to change in definition of wind exposed municipalities with respect to an IDS. First, Table E1 shows that our main findings are robust to alternative definitions of downwind exposure. Defining exposure as the number of IDS from which a municipality is downwind (intensive margin), as a dummy for being downwind from at least one IDS, as a dummy for above-average downwind exposure, or as a dummy for above-median downwind exposure still yields positive and statistically significant coefficients. These results suggest that our findings are not mechanically driven by the functional form relationship between our baseline treatment variable and cancer mortality. The results presented in Columns (2) and (3) of Table E1, in which we estimate a standard Difference-in-Differences with a binary treatment variable, also allow to circumvent the concerns raised by Callaway et al. (2024) about the additional assumptions that are required when estimating a Difference-in-Differences model with a continuous treatment variable.

Second, we provide evidence that our results do not depend on the choices that we made to approximate the historical wind trajectory connecting each IDS with nearby municipalities. In Table E2, we redefine $WI_{s,j,t}$ to take value 1 if the angle (θ) between the vector linking the IDS to the meteorological station and the wind direction vector

falls within $[0, 30°]$, $[0, 60°]$, $[0, 90°]$, or $[0, 120°]$. The results are considerably broadly coherent with out baseline method – which relies on Qiu et al. (2024) – and statistically significant up to 90°.

Biennial regression results. To further test our parallel trends assumption, we conduct a complementary exercise. We re-estimate the event-study specification by collapsing the data at the biennial level. Figure E3 reports the results, which confirm the absence of systematic pre-trends and that the post-period effect emerges gradually and persists over time.

Robustness to the inclusion of further covariates interacted with year dummies. Table E3 shows that our results remain statistically significant and similar in magnitude when altering the set of control variable to include all variables used to perform the balancing test presented in Figure A3, interacted with year fixed effects.

Robustness to the inclusion of large municipalities. Table E4 documents that our results are not sensitive to the exclusion of the two most populated cities of the Campania region (Naples and Salerno) while Table E5 documents that our results remain unaffected when including all five province capitals.

Robustness to restricting the sample only to municipalities officially recognized as a part of the Land of Fires. Table E6 restricts our the sample to 90 municipalities that have been officially recognized by the Italian Government as being part of the Land of Fires territory. Although the sample size used to perform this exercise is significantly smaller compared to our baseline sample, the estimates remain positive and statistically significant. The estimates are also much larger in magnitude, suggesting stronger effects in most exposed locations.

Robustness to accounting for correlation across time and space in cancer types. A potential concern with our results is that our aggregate effects could be inflated by correlated movements in time and space across different cancer types. To address this concern, we split all malignant tumors into three main categories: (i) hematological and reproductive cancers, (ii) digestive and respiratory cancers, and (iii) neurological, endocrine, and other cancers. For each municipality, we compute pairwise Pearson correlations across these three categories using only pre-treatment years (1980–1986). Then, we include these pre-period correlation measures (interacted with year dummies) as additional controls in our main regressions. Figure E4 shows that the results remain unchanged, suggesting that our estimates are not driven by pre-existing comovement across cancer categories.

Robustness to weighting observations proportionally to the municipality's population. In Figure E5, we estimate our main specification using Weighted Least Squares (WLS) with alternative population-based weights. Specifically, the top-left panel weights observations by the 1981 census population, while the top-right panel uses the 1991 census population. The bottom-left panel weights instead for the time-varying population measured at 1981, 1991, 2001, and 2011 censuses, respectively. Lastly, the bottom-right panel weights our main specification by the time-varying annual population estimates provided by the National Institute of Statistics. The conclusions remain unaltered.

Robustness to controlling for population dynamics. A potential concern with our results is that we may be comparing municipalities that are on different population growth trajectories during the years in our sample. In Figure E6, we assess that downwind municipalities did not experience differential trajectories of annual population growth rate relative to upwind municipalities. The event-study coefficients are small, statistically indistinguishable from zero, and do not display systematic pre-trends or persistent post-treatment divergences. Consistently, Table E9 shows that our main results are unaffected when we further control for the annual population growth rate in the main specification.[35] Taken together, these results mitigate potential concerns that our findings are driven by selective migration, demographic sorting, or broader population reallocation across municipalities over time, rather than by the effect of pollutant exposure on place-based cancer mortality.

Pseudo-Poisson maximum likelihood estimates. In Table E7, we report the estimates obtained when estimating a Pseudo-Poisson maximum likelihod model. This test is useful to rule out the possibility that our results are confounded by the estimation of a linear model using as the dependent variable a measure experiencing a non-negligible number of zeros. Although this concern is unlikely to be worrisome because we observe 0 cancer deaths in less than 5 percent of municipality-year observations, it is reassuring that the results presented in Table E7 confirm the pattern documented in the main results.

Standard errors robust to heteroskedasticity, autocorrelation, and spatial correlation. Table E10 assesses that our inference conclusions are not altered when taking into account the possibility of spatial correlation in the error terms $\varepsilon_{i,t}$. To this end, we compute Conley-HAC standard errors, using maximum cutoffs of 300 km for spatial

[35] The time-varying population growth rate might be a *bad control* since it is a potential outcome of exposure to pollutants – either because of the direct impact of cancer deaths on population growth or through other channels such as migration patterns. Nevertheless, we argue that documenting that our estimates are not affected by its inclusion is informative about the overall validity of our empirical analysis.

distance and 43 years for temporal lags (Conley, 1999).

Figure E1: Robustness Test I: Placebo (Non-Cancer causes of death)

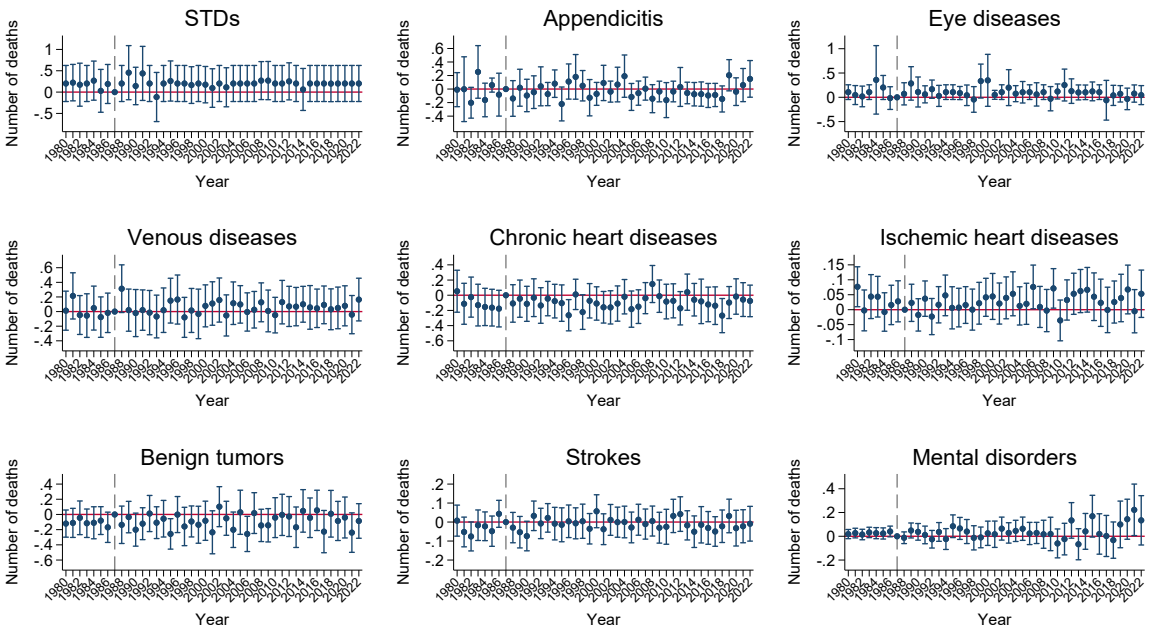

Notes: This figure reports falsification tests for the effect of downwind exposure to Illegal Disposal Sites (IDS) on the number of deaths from causes unrelated to the Land of Fires in Campania's municipalities, relative to 1987. Each panel shows a separate cause-of-death category (sexual transmitted diseases, appendicitis, eye diseases, venous disorders such as thrombosis and phlebitis, chronic heart diseases, ischemic heart diseases, benign tumors, strokes, mental disorders). Each cause of death is classified according to the International Classification of Diseases (ICD-9 up to 2003, ICD-10 from 2003 onwards in the ISTAT dataset): sexually transmitted diseases (0900-0999 and A50–A64), appendicitis (5400-5430 and K35-K38), eye diseases (3600-3799 and H00-H59), venous disorders (4510-4599 and I80-I89), chronic heart diseases (3930-3989 and I05-I09), ischemic heart diseases (4100-4149 and I20-I25), benign tumors (2100-2299 and D10-D36), strokes (4300-4380 and I60-I69), mental disorders (2900-3199 and F00-F99). Estimated equation is (1). The dashed gray vertical line (1987) marks the omitted year. To ensure that the estimates are comparable across specifications, we standardize all dependent variables to have mean 0 and standard deviation equal 1. 95% confidence intervals are based on standard errors robust to clustering at the municipality level.

Figure E2: Robustness Test II: Placebo (Non-Natural causes of death)

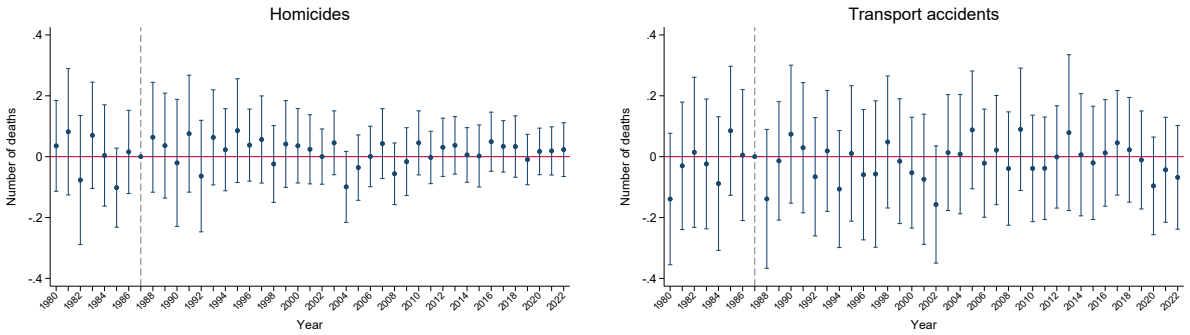

(a) Homicides (b) Transport accidents

Notes: This figure reports falsification tests for the effect of downwind exposure to Illegal Disposal Sites (IDS) on the number of deaths from homicides (panel a) and transport accidents (panel b). Each cause of death is classified according to the International Classification of Diseases (ICD-9 up to 2003, ICD-10 from 2003 onwards in the ISTAT dataset): homicides (E960-E969 and X85-Y09, Y87), transport accidents (E800-E848 and V01-V99). Estimated equation is (1). The dashed gray vertical line (1987) marks the omitted year. To ensure that the estimates are comparable across specifications, we standardize all dependent variables to have mean 0 and standard deviation equal 1. 95% confidence intervals are based on standard errors robust to clustering at the municipality level.

Figure E3: Robustness Test III: Biannual data

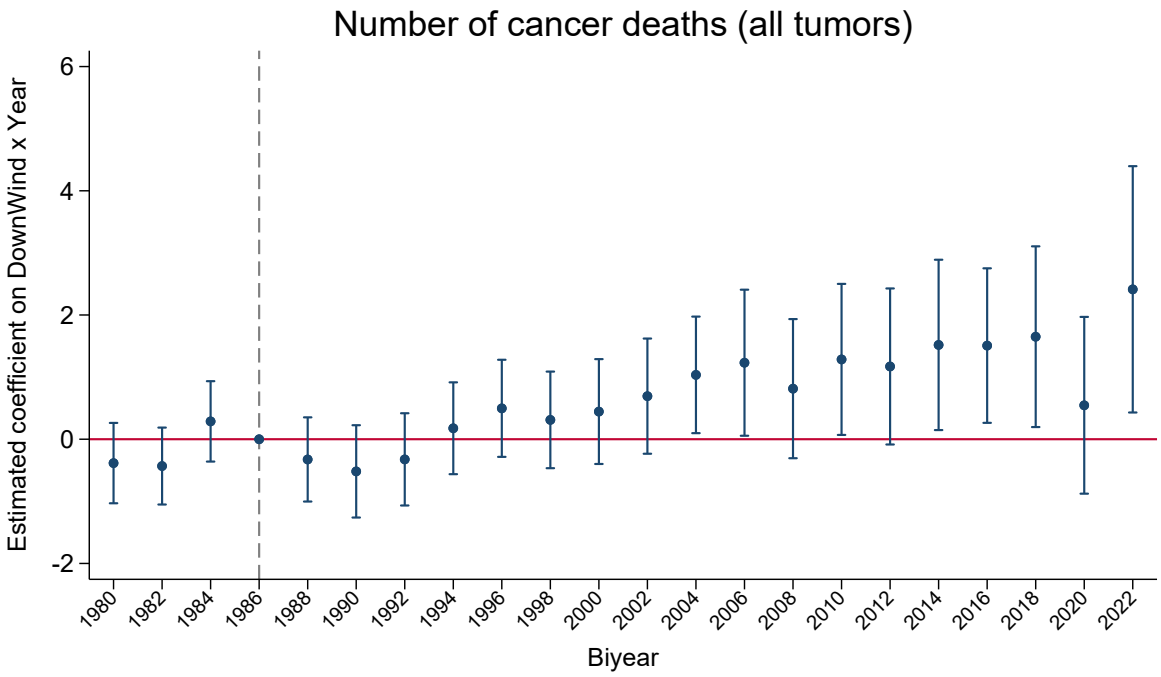

Notes: This figure reports coefficients for $\beta_{1980,\ldots,2022}$ in equation (1). Estimated equation is (1). Calendar years are grouped into two-year bins. The dashed gray vertical line marks the omitted reference biennium. 95% confidence intervals are based on standard errors robust to clustering at the municipality level.

Figure E4: Robustness Test IV: Controlling for pre-treatment correlation across cancer types

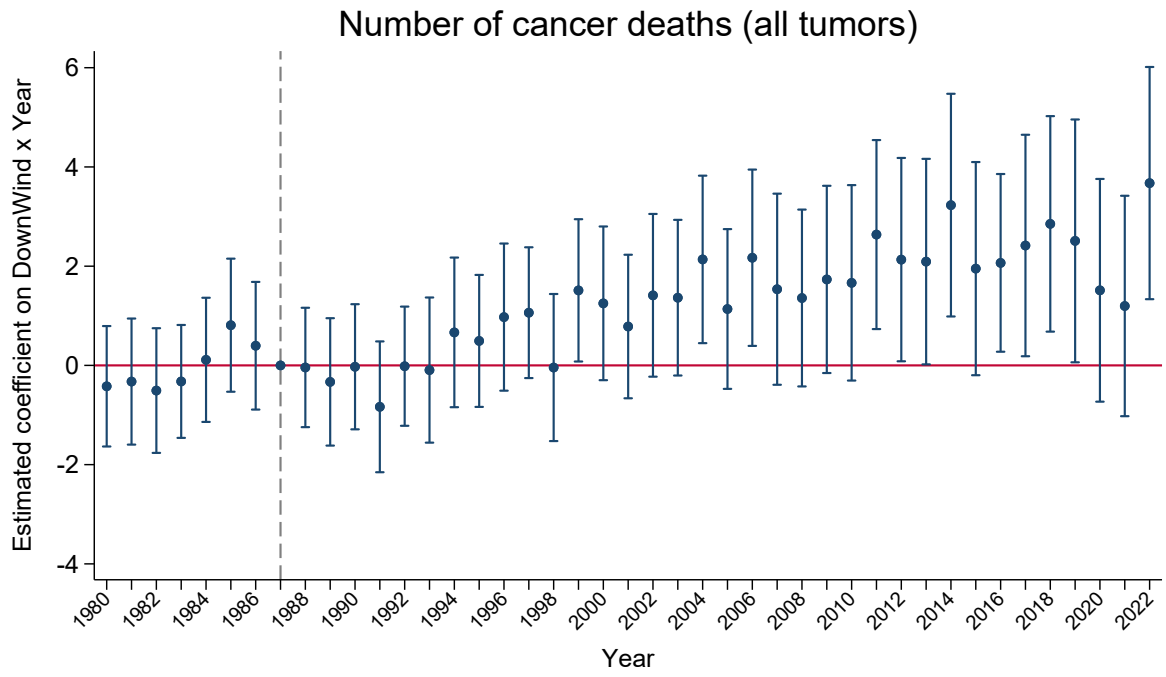

Notes: This figure reports coefficients for $\beta_{1980,\ldots,2022}$ in equation (1). Coefficient β_{1987} is omitted as it is considered the reference year. Estimated equation is (1) to which we add three municipality-level controls interacted with year dummies that capture pre-treatment (1980–1986) pairwise correlations between cancer categories: (i) hematological/reproductive vs. digestive/respiratory, (ii) hematological/reproductive vs. neurological/endocrine/other, and (iii) digestive/respiratory vs. neurological/endocrine/other. The dashed gray vertical line (1987) marks the omitted year. 95% confidence intervals are based on standard errors robust to clustering at the municipality level.

Table E1: Robustness Test V: Alternative definitions of downwind exposure

	(1)	(2)	(3)	(4)
	Number of cancer deaths (all tumors)			
DownWind (number) × Post	0.310*			
	(0.186)			
DownWind (dummy) × Post		1.180***		
		(0.406)		
DownWind (above average) × Post			4.111***	
			(1.206)	
Downwind (above median) × Post				2.612***
				(0.698)
Total number of IDS × Post	-0.116	0.00697	-0.0874	-0.0379
	(0.0932)	(0.0537)	(0.0646)	(0.0582)
Municipality FE	✓	✓	✓	✓
Year FE	✓	✓	✓	✓
Year FE × Surface	✓	✓	✓	✓
Year FE × Geographical characteristics	✓	✓	✓	✓
Year FE × Census population (1981)	✓	✓	✓	✓
Year FE × Province FE	✓	✓	✓	✓
Year FE × Organized crime controls	✓	✓	✓	✓
Observations	23294	23294	23294	23294
Dep var mean	15.70	15.70	15.70	15.70
R-squared	0.958	0.958	0.958	0.958
F-stat	1759.5	1599.6	1997.0	1840.5

Notes: Each column refers to a 3 km buffer radius from the IDS center, while varying the definition of downwind exposure. Column (1) defines the treatment variable as the number of nearby IDS relative to which the municipality is located downwind (intensive margin). Column (2) defines the treatment variable as a binary indicator equal to one if there is at least one nearby IDS from which the municipality is located downwind. Column (3) defines the treatment variable as a binary indicator equal to one if the number of IDS relative to which the municipality is located downwind exceeds the average number in the sample. Column (4) defines the treatment variable as a binary indicator equal to one if the number of IDS relative to which the municipality is located downwind exceeds the median number in the sample. Each column includes municipality and year fixed effects to account for time-invariant unobserved heterogeneity at the local level and common time shocks, while controlling for the total number of IDS. Each column also includes municipality surface, province fixed effects, minimum altitude as well as historical wind speed and rainfall (2001-2009), each of them fully interacted with year dummies. Each column also adds census population at baseline in 1981 (interacted with year dummies), as well as organized crime controls interacted with year dummies (number of civilians killed by the Mafia and a dummy equal to 1 if the municipality was dissolved for Mafia infiltration). Heteroskedasticity and cluster-robust standard errors at the municipality level are in parentheses. Stars indicate significance levels (* $p < 0.1$, ** $p < 0.05$, *** $p < 0.01$).

Table E2: Robustness Test VI: Alternative definition of $WI_{s,j,\tau}$ and $DownWind_i$ (θ)

	(1)	(2)	(3)	(4)
	Number of cancer deaths (all tumors)			
	$\theta = 30°$	$\theta = 60°$	$\theta = 90°$	$\theta = 120°$
DownWind × Post	1.816*	0.880**	0.870**	0.401
	(1.029)	(0.442)	(0.368)	(0.321)
Total number of IDS × Post	0.0252	0.0270	0.0229	0.0245
	(0.0512)	(0.0509)	(0.0510)	(0.0517)
Municipality FE	✓	✓	✓	✓
Year FE	✓	✓	✓	✓
Year FE × Surface	✓	✓	✓	✓
Year FE × Province FE	✓	✓	✓	✓
Year FE × Geographical characteristics	✓	✓	✓	✓
Year FE × Census population (1981)	✓	✓	✓	✓
Year FE × Organized crime controls	✓	✓	✓	✓
Observations	23294	23294	23294	23294
Dep var mean	15.70	15.70	15.70	15.70
R-squared	0.958	0.958	0.958	0.958
F-stat	1729.3	1673.5	1664.5	1814.1

Notes: Each column refers to a 3 km buffer radius from the IDS center, while varying both the computation of historical average wind direction at each IDS and $DownWind_i$. $WI_{s,j,t}$ equals 1 as the angle (θ) between the connection vector (vector linking the meteorological station to the IDS) and the wind direction vector falls within $[0, 30°]$, $[0, 60°]$, $[0, 90°]$, or $[0, 120°]$. An IDS is classified as upwind relative to the municipality's demographic centroid if the angle (θ) between the connection vector (line from the IDS to the demographic centroid) and the historical average wind direction ($\overline{WINDDIR_s}$) falls within the range $[0, 30°]$, $[0, 60°]$, $[0, 90°]$, or $[0, 120°]$. "Demographic" centroids are defined in Appendix D. The range $[0, 90°]$ corresponds to our main specification reported in Table 1. Each column includes municipality and year fixed effects to account for time-invariant unobserved heterogeneity at the local level and common time shocks, while controlling for the total number of IDS. Each column also includes municipality surface, province fixed effects, minimum altitude as well as historical wind speed and rainfall (2001-2009), each of them fully interacted with year dummies. Each column also adds census population at baseline in 1981 (interacted with year dummies), as well as organized crime controls interacted with year dummies (number of civilians killed by the Mafia and a dummy equal to 1 if the municipality was dissolved for Mafia infiltration). Heteroskedasticity and cluster-robust standard errors at the municipality level are in parentheses. Stars indicate significance levels (* $p < 0.1$, ** $p < 0.05$, *** $p < 0.01$).

Table E3: Robustness Test VII: Additional control variables

	(1)	(2)	(3)	(4)
	Number of cancer deaths (all tumors)			
DownWind × Post	0.870**	0.957**	0.772**	0.618*
	(0.368)	(0.379)	(0.363)	(0.360)
Total number of IDS × Post	0.0229	0.0128	0.00959	-0.0249
	(0.0510)	(0.0504)	(0.0499)	(0.0459)
Municipality FE	✓	✓	✓	✓
Year FE	✓	✓	✓	✓
Year FE × Surface	✓	✓	✓	✓
Year FE × Geographical characteristics	✓	✓	✓	✓
Year FE × Census population (1981)	✓	✓	✓	✓
Year FE × Province FE	✓	✓	✓	✓
Year FE × Organized crime controls	✓	✓	✓	✓
Year FE × Historical weather variables		✓	✓	✓
Year FE × Average wind direction			✓	✓
Year FE × Socio-demographic controls				✓
Observations	23294	23294	23294	23294
Dep var mean	15.70	15.70	15.70	15.70
R-squared	0.958	0.960	0.960	0.962

Notes: This table shows difference-in-differences estimates of the effect of wind exposure to IDS on the number of deaths by all malignant cancers from 1980 to 2022. Each column refers to a 3 km buffer radius from the IDS center (see Figure A2). The treatment is given by $DownWind_i$, defined as the ratio between the number of close IDS from which wind would transport pollutants towards municipality i and the total number of IDS close to i. The post-treatment period is identified by the indicator variable *Post*, which equals 1 for all years after 1987, and 0 otherwise. Column (1) presents results from the main specification reported in equation (2). Columns (2)-(4) progressively introduce all controls shown in the balancing test, each fully interacted with year dummies. Column (2) adds historical average temperature and humidity (2001-2009), as well as radon levels in year 2007. Column (3) includes historical average wind direction at the municipality level over 2001-2009. Column (4) further adds historical average taxable income per capita over 2000-2012, as well as socio-demographic controls from 1991 census: share of men, share of young population, share of elderly population, share of higher educated individuals, unemployment rate, employment rates in agriculture and health sectors, shares of large families and foreign residents. Heteroskedasticity and cluster-robust standard errors at the municipality level are in parentheses. Stars indicate significance levels (* $p < 0.1$, ** $p < 0.05$, *** $p < 0.01$).

Table E4: Robustness Test VIII: Excluding only Naples and Salerno

	(1)	(2)	(3)	(4)	(5)
	Number of cancer deaths (all tumors)				
DownWind × Post	1.794**	1.823**	0.992**	1.047***	0.999***
	(0.899)	(0.887)	(0.401)	(0.403)	(0.385)
Total number of IDS × Post	0.661***	0.489***	0.0543	0.0572	0.0170
	(0.0806)	(0.0747)	(0.0440)	(0.0437)	(0.0512)
Municipality FE	✓	✓	✓	✓	✓
Year FE	✓	✓	✓	✓	✓
Year FE × Surface	✓	✓	✓	✓	✓
Year FE × Geographical characteristics		✓	✓	✓	✓
Year FE × Census population (1981)			✓	✓	✓
Year FE × Province FE				✓	✓
Year FE × Organized crime controls					✓
Observations	23423	23423	23423	23423	23423
Dep var mean	16.42	16.42	16.42	16.42	16.42
R-squared	0.920	0.928	0.960	0.961	0.962
F-stat	5.245	4.449	104.7	185.1	1633.4

Notes: Column (1) presents a baseline model with municipality and year fixed effects to account for time-invariant unobserved heterogeneity at the local level and common time shocks, while controlling for the total number of IDS. It also includes municipality surface (interacted with year dummies). Columns (2)-(5) progressively introduce controls fully interacted with year dummies. Column (2) includes minimum altitude as well as historical average rainfall and wind speed (2001-2009). Column (3) adds census population at baseline (1981). Column (4) includes province fixed effects. Column (5) further adds organized crime controls (number of civilians killed by the Mafia and a dummy equal to 1 if the municipality was dissolved for Mafia infiltration). Heteroskedasticity and cluster-robust standard errors at the municipality level are in parentheses. Stars indicate significance levels (* $p < 0.1$, ** $p < 0.05$, *** $p < 0.01$).

Table E5: Robustness Test IX: Including all municipalities

	(1)	(2)	(3)	(4)	(5)
	Number of cancer deaths (all tumors)				
DownWind × Post	5.246*	5.734*	1.476**	1.387**	1.300**
	(2.890)	(3.293)	(0.630)	(0.585)	(0.568)
Total number of IDS × Post	0.774***	0.560***	0.289***	0.253***	0.160***
	(0.146)	(0.114)	(0.0487)	(0.0469)	(0.0536)
Municipality FE	✓	✓	✓	✓	✓
Year FE	✓	✓	✓	✓	✓
Year FE × Surface	✓	✓	✓	✓	✓
Year FE × Geographical characteristics		✓	✓	✓	✓
Year FE × Census population (1981)			✓	✓	✓
Year FE × Province FE				✓	✓
Year FE × Organized crime controls					✓
Observations	23509	23509	23509	23509	23509
Dep var mean	21.73	21.73	21.73	21.73	21.73
R-squared	0.989	0.990	0.997	0.997	0.997
F-stat	3.761	3.732	9873.8	14283.4	134401.3

Notes: Column (1) presents a baseline model with municipality and year fixed effects to account for time-invariant unobserved heterogeneity at the local level and common time shocks, while controlling for the total number of IDS. It also includes municipality surface (interacted with year dummies). Columns (2)-(5) progressively introduce controls fully interacted with year dummies. Column (2) includes minimum altitude as well as historical average wind speed and rainfall (2001-2009). Column (3) adds census population at baseline (1981). Column (4) includes province fixed effects. Column (5) further adds organized crime controls (number of civilians killed by the Mafia and a dummy equal to 1 if the municipality was dissolved for Mafia infiltration). Heteroskedasticity and cluster-robust standard errors at the municipality level are in parentheses. Stars indicate significance levels (* $p < 0.1$, ** $p < 0.05$, *** $p < 0.01$).

Table E6: Robustness Test X: Official Land of Fires area

	(1)	(2)	(3)	(4)
	Number of cancer deaths (all tumors)			
DownWind × Post	51.17**	55.62**	14.13*	14.67*
	(23.28)	(22.47)	(7.449)	(7.775)
Total number of IDS × Post	-0.246	0.395	-0.100	-0.0884
	(0.306)	(0.404)	(0.135)	(0.138)
Municipality FE	✓	✓	✓	✓
Year FE	✓	✓	✓	✓
Year FE × Surface	✓	✓	✓	✓
Year FE × Geographical characteristics	✓	✓	✓	✓
Year FE × Province FE		✓	✓	✓
Year FE × Census population (1981)			✓	✓
Year FE × Organized crime controls				✓
Observations	3826	3826	3826	3826
Dep var mean	66.97	66.97	66.97	66.97
R-squared	0.997	0.997	0.999	0.999

Notes: This table shows difference-in-differences estimates of the effect of wind exposure to IDS on the number of deaths by all malignant cancers from 1980 to 2022. Each column refers to a 3 km buffer radius from the IDS center (see Figure A2). The treatment is given by $DownWind_i$, defined as the ratio between the number of close IDS from which wind direction would transport pollutants towards municipality i and the total number of IDS close to i. The post-treatment period is identified by the indicator variable *Post*, which equals 1 for all years after 1987, and 0 otherwise. Column (1) presents a baseline model with municipality and year fixed effects to account for time-invariant unobserved heterogeneity at the local level and common time shocks, while controlling for the total number of IDS. It also includes municipality surface as well as minimum altitude, historical average wind speed and rainfall over 2001-2009 (each of them interacted with year dummies). Columns (2)-(4) progressively introduce controls fully interacted with year dummies. Column (2) includes province fixed effects. Column (3) adds census population at baseline (1981). Column (4) further includes organized crime controls (number of civilians killed by the Mafia and a dummy equal to 1 if the municipality was dissolved for Mafia infiltration). We restrict the sample to municipalities officially classified as part of the Land of Fires area (90 municipalities). The effective sample size is 89 municipalities due to administrative harmonization: Massa di Somma is merged into Cercola, as of 1980 boundaries. Heteroskedasticity and cluster-robust standard errors at the municipality level are in parentheses. Stars indicate significance levels (* $p < 0.1$, ** $p < 0.05$, *** $p < 0.01$).

Table E7: Robustness Test XI: Pseudo-Poisson maximum likelihood

	(1)	(2)	(3)	(4)	(5)
	Number of cancer deaths (all tumors)				
DownWind × Post	0.0769*	0.0729*	0.0693*	0.0695*	0.0578*
	(0.0400)	(0.0403)	(0.0376)	(0.0371)	(0.0341)
Total number of IDS × Post	0.00383*	0.00260	0.00486***	0.00574***	0.00451***
	(0.00200)	(0.00158)	(0.00141)	(0.00150)	(0.00144)
Municipality FE	✓	✓	✓	✓	✓
Year FE	✓	✓	✓	✓	✓
Year FE × Surface	✓	✓	✓	✓	✓
Year FE × Geographical characteristics		✓	✓	✓	✓
Year FE × Census population (1981)			✓	✓	✓
Year FE × Province FE				✓	✓
Year FE × Organized crime controls					✓
Observations	23294	23294	23294	23294	23294
Dep var mean	15.70	15.70	15.70	15.70	15.70
Pseudo R-squared	0.813	0.815	0.816	0.817	0.817
Chi-squared	108.5	851.1	1354.5	5714.9	104636.6

Notes: Column (1) presents a baseline model with municipality and year fixed effects to account for time-invariant unobserved heterogeneity at the local level and common time shocks, while controlling for the total number of IDS. It also includes the natural logarithm of municipality surface (interacted with year dummies). Columns (2)–(5) progressively introduce controls fully interacted with year dummies. Column (2) includes minimum altitude as well as historical wind speed and rainfall (2001-2009). Column (3) adds census population at baseline (1981). Column (4) includes province fixed effects. Column (5) further adds organized crime controls (number of civilians killed by the Mafia and a dummy equal to 1 if the municipality was dissolved for Mafia infiltration). Heteroskedasticity and cluster-robust standard errors at the municipality level are in parentheses. Stars indicate significance levels (* $p < 0.1$, ** $p < 0.05$, *** $p < 0.01$).

Table E8: Robustness Test XII: PPML estimates with baseline population exposure

	(1)	(2)	(3)	(4)
	Cancer mortality			
DownWind × Post	0.0853**	0.0736*	0.0772*	0.0759*
	(0.0433)	(0.0417)	(0.0400)	(0.0407)
Total number of IDS × Post	0.00444**	0.00267*	0.00241	0.00211
	(0.00193)	(0.00157)	(0.00159)	(0.00169)
Municipality FE	✓	✓	✓	✓
Year FE	✓	✓	✓	✓
Year FE × Surface	✓	✓	✓	✓
Census population (1981) exposure	✓	✓	✓	✓
Year FE × Geographical characteristics		✓	✓	✓
Year FE × Province FE			✓	✓
Year FE × Organized crime controls				✓
Observations	23294	23294	23294	23294
Dep var mean	15.70	15.70	15.70	15.70
Pseudo R-squared	0.813	0.815	0.816	0.816
Chi-squared	180.0	976.1	3748.1	16558.9

Notes: The dependent variable is the annual number of cancer deaths for all tumors. PPML estimates include 1981 municipality population as an exposure term, so coefficients are interpreted relative to baseline population rather than raw death counts. Column (1) presents a baseline model with municipality and year fixed effects to account for time-invariant unobserved heterogeneity at the local level and common time shocks, while controlling for the total number of IDS. It also includes municipality surface (interacted with year dummies). Columns (2)–(4) progressively introduce controls fully interacted with year dummies. Column (2) includes minimum altitude as well as historical wind speed and rainfall (2001-2009). Column (3) adds province fixed effects. Column (4) further includes organized crime controls (number of civilians killed by the Mafia and a dummy equal to 1 if the municipality was dissolved for Mafia infiltration). Heteroskedasticity and cluster-robust standard errors at the municipality level are in parentheses. Stars indicate significance levels (* $p < 0.1$, ** $p < 0.05$, *** $p < 0.01$).

Figure E5: Robustness Test XIII: Weighting for census population (WLS)

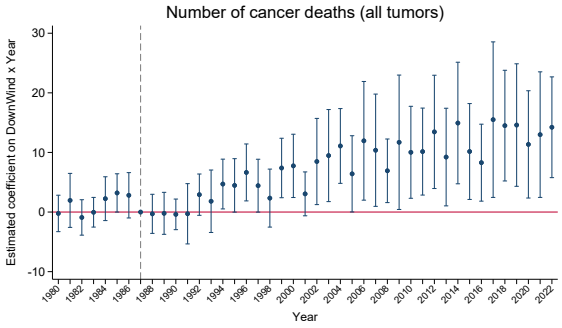

(a) Weight: Census 1981

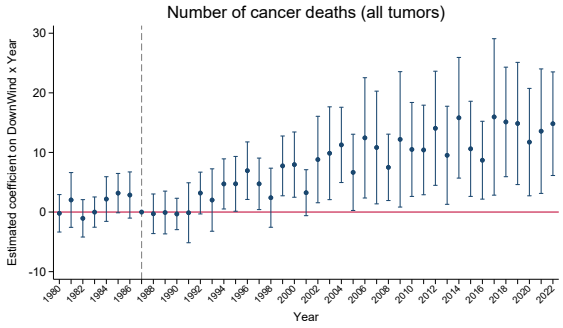

(b) Weight: Census 1991

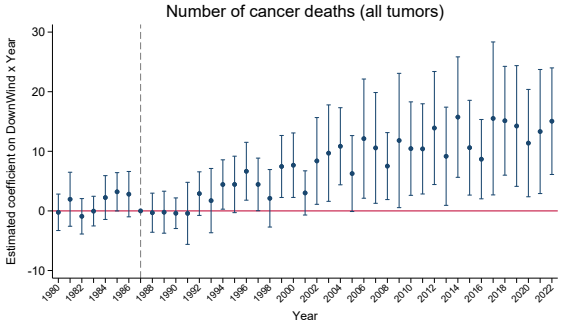

(c) Weight: Censuses 1981–2011

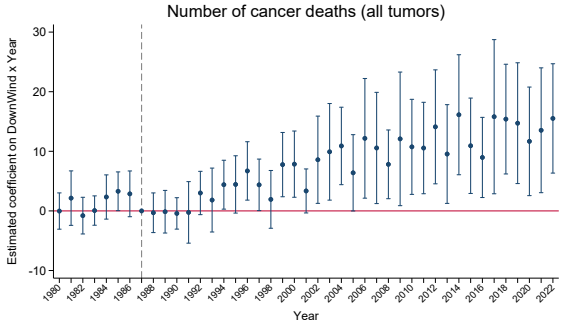

(d) Weight: Annual Population

Notes: This figure reports coefficients for $\beta_{1980,\ldots,2022}$ from equation (1), re-estimated by Weighted Least Squares (WLS) using alternative population-based weights. Weights are based on: (i) 1981 census population, (ii) 1991 census population, (iii) time-varying census population (1981, 1991, 2001 and 2011), and (iv) time-varying annual population estimates provided by the National Institute of Statistics. Estimated equation is (1). The dashed gray vertical line marks the omitted year. 95% confidence intervals are based on standard errors robust to clustering at the municipality level.

Figure E6: Robustness Test XIV: Wind Exposure and Population Growth Rate

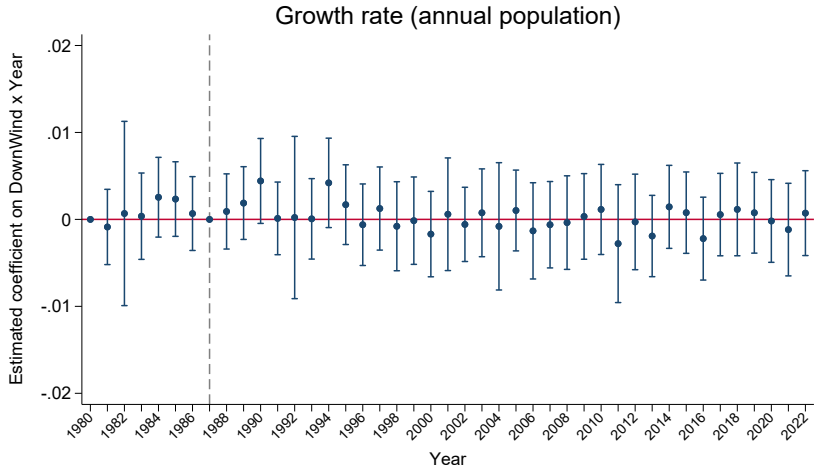

Notes: This figure reports coefficients for $\beta_{1980,\ldots,2022}$ in equation (1), where the dependent variable is the annual population growth rate estimated by ISTAT. Coefficient β_{1987} is omitted as it is considered the reference year. Estimated equation is (1). The dashed gray vertical line (1987) marks the omitted year. 95% confidence intervals are based on standard errors robust to clustering at the municipality level.

Table E9: Robustness Test XV: Controlling for Population Growth Rate

	(1)	(2)	(3)	(4)	(5)	(6)
	Number of cancer deaths (all tumors)					
DownWind × Post	1.417*	1.477*	0.812**	0.873**	0.815**	0.807**
	(0.814)	(0.806)	(0.394)	(0.394)	(0.370)	(0.368)
Total number of IDS × Post	0.624***	0.451***	0.0535	0.0631	0.0188	0.0149
	(0.0761)	(0.0696)	(0.0458)	(0.0444)	(0.0512)	(0.0514)
Municipality FE	✓	✓	✓	✓	✓	✓
Year FE	✓	✓	✓	✓	✓	✓
Year FE × Surface	✓	✓	✓	✓	✓	✓
Year FE × Geographical characteristics		✓	✓	✓	✓	✓
Year FE × Census population (1981)			✓	✓	✓	✓
Year FE × Province FE				✓	✓	✓
Year FE × Organized crime controls					✓	✓
Population growth rate						✓
Observations	22754	22754	22754	22754	22754	22754
Dep var mean	15.88	15.88	15.88	15.88	15.88	15.88
R-squared	0.917	0.927	0.956	0.957	0.959	0.959
F-stat	5.032	4.525	65.79	135.4	1279.2	1100.3

Notes: Column (1) presents a baseline model with municipality and year fixed effects to account for time-invariant unobserved heterogeneity at the local level and common time shocks, while controlling for the total number of IDS. It also includes municipality surface (interacted with year dummies). Columns (2)-(5) progressively introduce controls fully interacted with year dummies. Column (2) includes minimum altitude as well as historical average wind speed and rainfall (2001-2009). Column (3) adds census population at baseline (1981). Column (4) includes province fixed effects. Column (5) further adds organized crime controls (number of civilians killed by the Mafia and a dummy equal to 1 if the municipality was dissolved for Mafia infiltration). Column (6) finally introduces the annual population growth rate. To ensure comparability with Table 1, year 1980 is excluded from all specifications. Heteroskedasticity and cluster-robust standard errors at the municipality level are in parentheses. Stars indicate significance levels (* $p < 0.1$, ** $p < 0.05$, *** $p < 0.01$).

Table E10: Robustness Test XVI: Conley HAC Standard Errors

	(1)	(2)	(3)	(4)	(5)
	Number of cancer deaths (all tumors)				
DownWind × Post	1.484**	1.545**	0.862***	0.926***	0.870***
	(0.690)	(0.675)	(0.320)	(0.321)	(0.302)
Total number of IDS × Post	0.643***	0.467***	0.0567	0.0666*	0.0229
	(0.0690)	(0.0624)	(0.0370)	(0.0358)	(0.0409)
Municipality FE	✓	✓	✓	✓	✓
Year FE	✓	✓	✓	✓	✓
Year FE × Surface	✓	✓	✓	✓	✓
Year FE × Geographical characteristics		✓	✓	✓	✓
Year FE × Census population (1981)			✓	✓	✓
Year FE × Province FE				✓	✓
Year FE × Organized crime controls					✓
Observations	23294	23294	23294	23294	23294
R-squared	0.0852	0.196	0.533	0.543	0.557

Notes: This table shows difference-in-differences estimates of the effect of wind exposure to IDS on the number of deaths by all malignant cancers from 1980 to 2022. Each column refers to a 3 km buffer radius from the IDS center (see Figure A2). The treatment is given by $DownWind_i$, defined as the ratio between the number of close IDS from which wind direction would transport pollutants towards municipality i and the total number of IDS close to i. The post-treatment period is identified by the indicator variable *Post*, which equals 1 for all years after 1987, and 0 otherwise. Each column replicates Table 1 while computing Conley-HAC standard errors with maximum cutoffs of 300 km for spatial distance and 43 years for temporal lags. Heteroskedasticity and Conley HAC standard errors at the municipality level are in parentheses. Stars indicate significance levels (* $p < 0.1$, ** $p < 0.05$, *** $p < 0.01$).